BIROn - Birkbeck Institutional Research Online

When did the Indus River of South-Central Asia take on its "modern" drainage configuration?

Yani Najman[1,†], Guangsheng Zhuang[1,2], Andrew Carter[3], Lorenzo Gemignani[4,*], Ian Millar[5], and Jan Wijbrans[4]
[1]*Lancaster Environment Centre, Lancaster University, Lancaster LA1 4YQ, UK*
[2]*Department of Geology and Geophysics, Louisiana State University, Baton Rouge, Louisiana 70803, USA*
[3]*Department of Earth and Planetary Sciences, Birkbeck College, University of London, London WC1E 7HX, UK*
[4]*Faculty of Earth and Life Science, Vrije Universiteit, 1081 HV Amsterdam, Netherlands*
[5]*Natural Environment Research Council, Isotope Geosciences Lab, British Geological Survey, Keyworth, Nottingham NG12 5GG, UK*

ABSTRACT

For sedimentary archives to be used as a record of hinterland evolution, the factors affecting the archive must be known. In addition to tectonics, a number of factors, such as changes in climate and paleodrainage, as well as the degree of diagenesis, influence basin sediments. The Indus River delta-fan system of South-Central Asia records a history of Himalayan evolution, and both the onshore and offshore sedimentary repositories have been studied extensively to research orogenesis. However, a number of unknowns remain regarding this system. This paper seeks to elucidate the paleodrainage of the Indus River, in particular when it took on its modern drainage configuration with respect to conjoinment of the main Himalayan (Punjabi) tributary system with the Indus trunk river. We leverage the fact that the Punjabi tributary system has a significantly different provenance signature than the main trunk Indus River, draining mainly the Indian plate. Therefore, after the Punjabi tributary system joined the Indus River, the proportion of Indian plate material in the repositories downstream of the confluence should have been higher than in the upstream repository. We compared bulk Sr-Nd data and detrital zircon U-Pb data from the Cenozoic upstream peripheral foreland basin and downstream Indus delta and Indus Fan repositories. We determined that throughout Neogene times, repositories be-

low the confluence had a higher proportion of material from the Indian plate than those above the confluence. Therefore, we conclude that the Indus River took on its current configuration, with the Punjabi tributary system draining into the Indus trunk river in the Paleogene, early in the history of the orogen. The exact time when the tributary system joined the Indus should correlate with a shift to more Indian plate input in the downstream repositories only. While the upstream repository records no change in Indian plate input from Eocene to Neogene times, a shift to increased material from the Indian plate occurs at the Eocene–Oligocene boundary in the delta, but sometime between 50 Ma and 40 Ma in the fan. Though further work is required to understand the discrepancy between the two downstream repositories, we can conclude that the tributary system joined the Indus trunk river at or before the start of the Oligocene.

1. INTRODUCTION

The Himalaya, the largest orogen on Earth, garners significant interest from researchers in a variety of disciplines. While considerable information on the mountain belt's evolution can be determined from its hard rock geology, its early history is often destroyed in these rocks by later tectonism, metamorphism, and/or erosion. In these circumstances, researchers turn to information recorded in the sedimentary archive of material eroded from the mountain belt and preserved in surrounding sedimentary basins, both onshore and offshore.

The main repositories of Himalayan detritus are preserved in the orogen's suture zone, peripheral and axial foreland basins onshore (e.g., Hodges, 2000; Najman, 2006; Shah, 2009), and the Indus and Bengal fans offshore, which

are the world's largest sediment fans (Nyberg et al., 2018). Detritus from all of these basins has been studied to document hinterland evolution using a variety of bulk-rock and single-grain analytical techniques. For example, studies of the Indus River's sedimentary repository include detrital feldspar Pb-isotopic analyses applied to the Indus Suture Zone molasse (Clift et al., 2001b), detrital zircon fission-track and Sm-Nd bulk analyses applied to the peripheral foreland basin sedimentary rocks (e.g., Chirouze et al., 2015), detrital zircon U-Pb analyses applied to the axial foreland basin (e.g., Zhuang et al., 2015), and heavy mineral and petrographic data (Andò et al., 2020; Garzanti et al., 2020) applied to the Indus Fan. However, for the sedimentary archives to be robustly interpreted, the evolution of the river's paleodrainage must be known, since significant changes in drainage affect the sedimentary archive. This paper focuses on reconstruction of the Lower Indus River paleodrainage.

Today, the Indus River flows west along the Indus Suture Zone that separates the Indian and Asian plates, before turning south across the Himalaya to eventually flow into the northern Indian Ocean, giving rise to the Indus Fan (Fig. 1). Here, we define the Lower Indus as that part of the Indus River downstream (south) of the Himalayan mountain front that flows axially, southward along the Indus Basin. We define the Upper Indus as that part of the Indus River that flows through the mountains and is subdivided into the "west-flowing axial Upper Indus," which flows westward from its headwaters, axially along the Indus Suture Zone, and, farther downstream, the "south-flowing transverse Upper Indus," which cuts southward across the mountain range (Fig. 1A). The main tributaries of the Indus are the Punjabi or Himalayan tributaries of the Jhelum, Chenab, Ravi, Beas, and Sutlej rivers, herein called the Punjabi tributary

https://doi.org/10.1130/B36596.1.
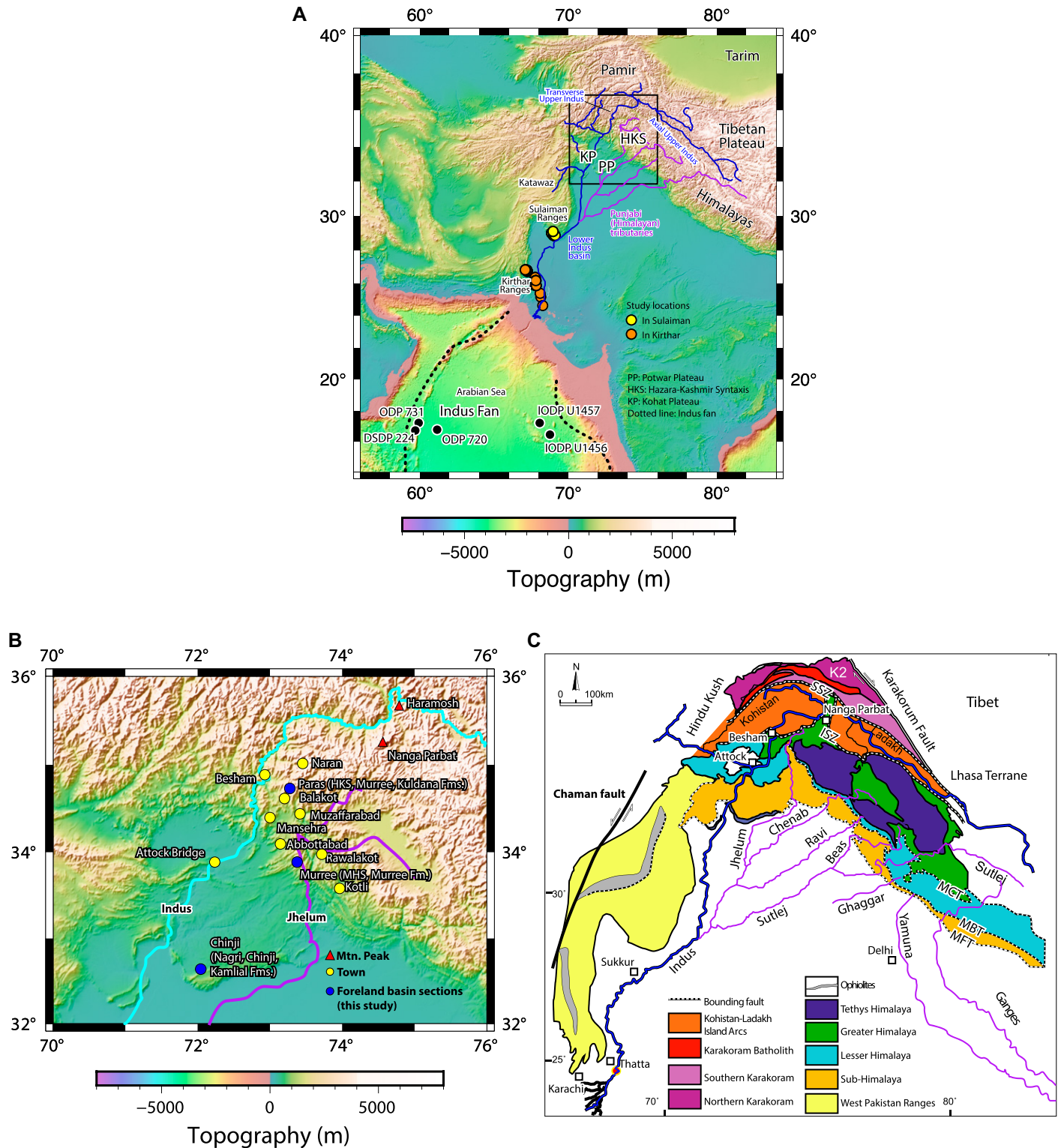
Figure 1. (A) Map showing modern drainage of the Indus River, South-Central Asia, with the Punjabi tributary system and the Indus Fan (black dotted line). Also shown are the onshore Lower Indus (Kirthar and Sulaiman) and offshore Integrated Ocean Drilling Program (IODP), Ocean Drilling Program (ODP), and Deep Sea Drilling Project (DSDP) locations of previously published data (Roddaz et al., 2011; Zhuang et al., 2015; Clift et al., 2001a, 2019; Clift and Blusztajn, 2005; Feng et al., 2021) with which we compared our new upstream data. Black rectangle shows the location of Figure 1B. (B) Locations of new data (this study) and various towns and sample sites discussed in the text. HKS—Hazara-Kashmir syntaxis; MHS—Murree Hill station. (C) Drainage superimposed on regional geology (Clift et al., 2019). ISZ—Indus Suture Zone; MBT—Main Boundary Thrust; MCT—Main Central Thrust; MFT—Main Frontal Thrust; SSZ—Shyok Suture Zone.

system, which predominantly drains the Indian plate (Fig. 1C).

Mid-Eocene Owen Ridge sediment is considered to be early Indus Fan material derived from north of the Indian plate (Clift et al., 2001a, 2002a). This places a lower bound on the timing of initiation of the Indus River, although its upstream configuration is debated. For the Upper Indus, the proposed time of its initiation as a river flowing westward along the suture zone ranges from early Eocene through Miocene (Bhattacharya et al., 2021; Clift et al., 2001b; Henderson et al., 2011; Najman, 2006; Sinclair and Jaffey, 2001).

This paper focuses on the evolution of paleodrainage of the Lower Indus River. Various suggestions have been made regarding whether western Himalayan rivers switched between flowing east to the Ganges and Bengal Fan catchment and west to the Indus River and Fan catchment. While a number of authors based their interpretations on paleocurrent data from the peripheral foreland basin deposits (e.g., see review in Burbank et al., 1996), Clift and Blusztajn (2005) used geochemical data from the Indus Fan. They considered that changes in the geochemical signature of the Indus Fan sediment archive after 5 Ma represent a major drainage change in the Lower Indus at this time, when the Punjabi tributaries of the Lower Indus River (Jhelum, Chenab, Ravi, and Sutlej rivers; Figs. 1A and 1C) switched from flowing eastward to the Ganges and Bengal Fan, to westward to the Indus River and Indus Fan. However, Chirouze et al. (2015) considered that this geochemical change could be better interpreted as the result of variations in upland exhumation. This suggestion was later agreed upon by the original proponents of the drainage diversion hypothesis (Clift et al., 2019; Zhou et al., 2021); thus, when the Indus River took on its current configuration with respect to the Punjabi tributary system remains unknown.

Using a rationale similar to that of Chirouze et al. (2015), we compare provenance indicators from upstream and downstream of the confluence of the Punjabi tributary system with those from the Indus River, and from this comparison we determine when a provenance change in the downstream repository is detected, and thus when the tributary system joined the Indus trunk river. We extend the peripheral foreland basin Sr-Nd dataset of Chirouze et al. (2015) from the mid-Miocene down section as far as the Eocene to determine when the provenance change occurred, and additionally we apply new provenance indicators, namely detrital zircon U-Pb ages and detrital white mica Ar-Ar ages.

2. BACKGROUND

2.1. Himalayan Geology

2.1.1. Tectonic Units

The Indus Suture Zone separates the Asian Lhasa Terrane to the north from the Indian plate to the south. In the west, the Kohistan-Ladakh intraoceanic island arc is sandwiched between the Indian and Asian plates, with the southern margin of the Asian plate at this location comprised of the Karakoram and Hindu Kush. The northern suture separating the Asian plate and Kohistan-Ladakh intraoceanic island arc is termed the Shyok Suture Zone, and the southern suture separating the Kohistan-Ladakh intraoceanic island arc and Indian plate is termed the Indus Suture Zone, also known as the Main Mantle Thrust in this region (Fig. 1C). The Indus River flows west along the Indus Suture Zone before turning south to cross the Himalaya and foreland basin before debouching into the Arabian Sea.

The Lhasa terrane comprises Phanerozoic low-grade metamorphic and sedimentary cover overlying Precambrian–Cambrian basement (e.g., Leier et al., 2007). Along its southern rampart, the Gangdese continental arc batholiths of the Trans-Himalaya are intruded, which represent the Andean-type southern margin of Asia prior to consumption of the intervening Neo-Tethys Ocean (Schärer et al., 1984). While Gangdese intrusions are Mesozoic–Paleogene in age, post-collisional igneous activity continued into Miocene times (Hodges, 2000). To the west, the Lhasa terrane terminates against the Karakoram Fault. West of the fault, the southern margin of Asia is represented by the Karakoram (Fig. 1C). The Karakoram terrane is divided into three units (Hildebrand et al., 1998, 2001; Searle et al., 1999): the Northern Karakoram Sedimentary Unit, the Southern Karakoram Metamorphic Belt, and the intervening Karakoram Batholith. The Northern Karakoram Sedimentary Unit comprises pre-Ordovician crystalline basement covered by an Ordovician to Cretaceous sedimentary succession (Gaetani and Garzanti, 1991; Gaetani et al., 1993; Zanchi and Gaetani, 2011). The Karakoram Batholith includes pre–India-Asia collision, Andean-type subduction-related granitoids, and post–India-Asia collisional leucogranites. The age of metamorphism of the Southern Karakoram Metamorphic Belt ranges from Late Cretaceous to late Miocene (Fraser et al., 2001; Palin et al., 2012; Searle et al., 2010).

The Kohistan-Ladakh intraoceanic island arc separates the Indian and Asian plates in the west of the orogen. It consists of Late Cretaceous and Eocene plutonic belts, and pyroxene granulites, calc-alkaline volcanics, amphibolites, and minor metasediments (Coward et al., 1984; Schaltegger et al., 2002), fringed by ophiolitic mélange in the southern suture (DiPietro et al., 2000; DiPietro and Pogue, 2004).

The Indian plate lies to the south of the Kohistan-Ladakh intraoceanic island arc. As summarized in Hodges (2000), in the central and eastern part of the orogen, the Indian plate Himalaya is divided, from north to south, into the Tethyan Himalaya, the Greater Himalaya, Lesser Himalaya, and Cenozoic foreland basin sedimentary rocks of the sub-Himalaya (Fig. 1C). Typically, the Tethyan Himalaya, separated from the Greater Himalaya to the south by the South Tibetan Detachment System, consists of Paleozoic–Mesozoic sedimentary and low-grade metasedimentary rocks that were deposited on the Tethyan Ocean passive margin. The Greater Himalaya, separated from the Lesser Himalaya to the south by the Main Central Thrust, consists predominantly of medium- to high-grade Neoproterozoic–Ordovician metamorphic rocks that were subjected to metamorphism and anatexis during the Cenozoic Himalayan orogeny, when they were intruded by Neogene leucogranites; and the Lesser Himalaya, separated from the Cenozoic sub-Himalaya foreland basin sedimentary rocks to the south by the Main Boundary Thrust, which consists of Paleoproterozoic metamorphosed and unmetamorphosed Indian plate rocks. These lithologies also broadly constitute the Indian plate Himalaya to the west in Pakistan. However, exact correlation is uncertain, the degree of metamorphism differs, and the lithologies are not structurally imbricated in the same way (Treloar et al., 2019). According to DiPietro and Pogue (2004), north of the Khairabad Thrust (MCT equivalent in Pakistan), metamorphosed rocks of ages equivalent to the Tethyan, Greater, and Lesser Himalaya are found, while both Lesser and Tethyan equivalents are found between the Khairabad Thrust and the Main Boundary Thrust. The Nanga Parbat syntaxis is considered to be of Lesser, Greater, and Tethyan Himalayan affinity (Argles et al., 2003). In this paper, we refer to the Neoproterozoic–Ordovician rocks as "Greater Himalayan lithological correlatives," the Paleoproterozoic rocks as "Lesser Himalayan lithological correlatives," and the Paleozoic–Mesozoic rocks as "Tethyan Himalayan lithological correlatives." Such terms do not reflect the locations of the rocks within the various thrust-bound terranes, as they do farther east.

The units described above have distinct zircon U-Pb ages and Nd isotopic signatures associated with different crustal evolutionary histories (e.g., Argles et al., 2003; Clift et al., 2019; DeCelles et al., 2004, 2016; Gehrels et al., 2011; Najman,

TABLE 1. COMPARISON OF PROVENANCE DATA FROM THE PERIPHERAL FORELAND BASIN WITH THOSE
FROM THE LOWER INDUS AXIAL BASIN AND INDUS FAN, SOUTH-CENTRAL ASIA

Terrane/basin stratigraphy	ε_{Nd}	Zircons (%) with U-Pb ages 200–40 Ma (arc-derived)
Source region characteristics*		
Karakoram	Average: −10	Dominant 200–40 Ma populations with some older grains to Precambrian
Kohistan island arc	Average: +5	Entirely 200–40 Ma
Indian plate	Average: −15 (GHS), −22 (LHS & NP), −11 (THS)	Near 100% older than 200 Ma
Upstream peripheral foreland basin		
Modern Indus River	*No data for downstream of GHS* At Skardu (upstream of GHS) −8.6[†] At Besham (just into GHS) −10.7[†]	At Attock: 53% arc[§]
Upper Miocene Nagri Formation	−9.4, −9.9	67% arc
Mid-Miocene Chinji Formation	−7.7, −8.7 (our data) −3.8 to −7.7 (Chirouze et al., 2015)	47% arc
Lower mid-Miocene Kamlial Formation	−8.3	51% arc
Lower Miocene Murree Formation	−13.8 (MHS) −8.1, −9.2 (HKS, Paras north of Balakot)	23% arc (MHS) 50% arc (HKS, Paras north of Balakot) 0%–4% arc (HKS, Balakot)[#] 0%–17% (HKS Muzaffarabad)[#]
Lower–mid-Eocene Kuldana Formation	−8.1, −8.8	49%–75% arc (HKS, Balakot)[#] 6%–74% arc (HKS, Muzaffarabad)[#] Qasim Murree Hill station 34%–78% arc (MHS)**
Downstream Lower Indus Axial Basin, Kirthar (K), and Sulaiman (S) regions		
Modern Indus River	−15 (below Sutlej confluence and at delta)[†]	At Thatta: 18% arc[††]
Pliocene Siwalik Group	−12 (K), n = 2[##]	12% arc (K)[##]
Upper Miocene Siwaliks	−9.3 (K), n = 1[##]	
Middle Miocene Siwalik Group & Vihowa Formation	−11 (K), n = 8[##]	22% arc (K)[##]
Lower Miocene Vihowa & Chitarwata formations	−10.5 (S), n = 2[§§] −13.1 (K), n = 5[##]	
Upper Oligocene Chitarwata Formation	Upper upper Oligocene: −11.1 (S), n = 3[§§] Lower upper Oligocene: −12.4 (S), n = 3[§§]	
Lower Oligocene Chitarwata Formation	−9.6 (S), n = 1[§§] −13.4 (K), n = 1[##]	16% arc (K)[##] 16% arc (S)[##]
Lower–mid-Eocene Ghazij and Kirthar Groups	Average: −9.3 (S), n = 2[§§] Average: −7.5 (K), n = 1[##]	
Indus Fan		
Pliocene	Average: −10.8, n = 8[†††]	19%–32%[§§§,****]
Miocene	Average: −10.1, n = 47[***,§§§,###]	11%–48%[§§§,###,****]
Oligocene	Average: −11.9, n = 16[***,§§§]	16%–43%[###]
Mid-Eocene	−11.96, −5.2***	
Early Eocene	−9.3[†††]	

Note: Source region signatures are also provided. Note that three "Mid-Eocene" data points from the Indus Fan are omitted as the age was noted as questionable in the original publication of Clift et al. (2001a). GHS, LHS, THS—Greater-, Lesser-, Tethyan Himalaya, respectively; NP—Nanga Parbat; MHS—Murree Hill station; HKS—Hazara-Kashmir syntaxis.

*Compiled source region data from Ahmad et al. (2000); Bignold and Treloar (2003); Clift et al. (2019); DeCelles et al. (2004, 2018); Deniel et al. (1987); Gehrels et al. (2011); Ji et al. (2009); Khan et al. (1997, 2004, 2009); Mahéo et al. (2009); Miller et al. (1999); Najman (2006); Pan et al. (2014); Richards et al. (2005); Robinson et al. (2001); Whittington et al. (1999); Zhang et al. (2004); Zhu et al. (2012); Zhuang et al. (2018), and additional references as listed in Figure S3B (see text footnote 1).

[†]Clift et al. (2002b).
[§]Alizai et al. (2011) and Clift et al. (2022).
[#]Ding et al. (2016b).
**Qasim et al. (2018).
[††]Clift et al. (2004).
[§§]Roddaz et al. (2011).
[##]Zhuang et al. (2015).
***Clift et al. (2001a).
[†††]Clift and Blusztajn (2005).
[§§§]Clift et al. (2019).
[###]Feng et al. (2021).
****Zhou et al. (2022).

2006). These differences (Table 1) allow for the use of these techniques as provenance indicators in the detrital record downstream (e.g., Clift et al., 2019; DeCelles et al., 2004, 2016; Gehrels et al., 2011; Najman, 2006).

The overwhelming majority of zircons from the Indian plate have U-Pb ages older than 400 Ma (DeCelles et al., 2004; Gehrels et al., 2011), with the minor exception of grains dated ca. 130 Ma from the Tethyan Himalaya (e.g., Clift et al., 2014) and Neogene grains eroded from leucogranites (e.g., Hodges, 2000, and references therein). Within the Indian plate, grains dated at 2300–1500 Ma are characteristic of the Lesser Himalaya, and those dated at 1250–300 Ma are characteristic of the Greater and Tethyan Himalaya, although not uniquely so (Clift et al., 2019). By contrast, zircons from the Kohistan-Ladakh intraoceanic island arc are exclusively aged at 200–40 Ma, while the southern Asian margin (the Karakoram terrane and the Lhasa terrane to the east) also has a high proportion of grains of such age, but also with some Neogene grains and older grains stretching to the Precambrian that are derived from the substrate into which the Mesozoic–Paleogene plutons intruded (e.g., Zhuang et al., 2018, and references therein).

The old continental crust of the Indian plate has a mean ε_{Nd} value of −15 for the Greater Himalaya, −22 for the Lesser Himalaya, and −11 for the Tethyan Himalaya (Ahmad et al., 2000; Deniel et al., 1987; Richards et al., 2005; Robinson et al., 2001; Zhang et al., 2004). By contrast, the Asian and intraoceanic arc terranes have more positive values that reflect the dominance of Mesozoic–Paleogene plutons: the Kohistan-Ladakh intraoceanic island arc has values of ∼+5 (Bignold and Treloar, 2003; Khan et al., 1997, 2004, 2009), while the Karakoram, which consists of both old sedimentary and metamorphic rocks as well as younger plutons, has an average value of ∼−9.6 (Mahéo et al., 2009; Miller et al., 1999). Data from the Lhasa terrane are mainly from the central and eastern part of the orogen: the Gangdese/Trans-Himalaya have values ranging from +0.9 to +5.5 for the Mesozoic granitoids and +2.4 to +8.5 for the Paleocene–Eocene granitoids, in contrast to the Oligocene–Miocene granitoids with values of −9.4 to +5.5 (Ji et al., 2009; Pan et al., 2014), while

the continental substrate into which these plutons intruded has an average recorded ε_{Nd} value of −9 (Pan et al., 2014; Zhu et al., 2009, 2012).

2.1.2. Tectonic Evolution

Prior to India-Asia collision, India was subducting beneath Asia as the Neo-Tethys Ocean closed, with the Kohistan-Ladakh intraoceanic island arc located between the two continents in the west. The timing of India-Asia collision, and whether the island arc collided with India or Asia first, is disputed; a majority of researchers consider India-Asia collision to have occurred around 60–55 Ma (see review in Hu et al., 2016, and references therein), with other estimates extending to ca. 35 Ma or 25–20 Ma (Aitchison et al., 2007; Bouilhol et al., 2013; van Hinsbergen et al., 2012).

The west differs from the better-studied east and central part of the orogen in both the presence of the Kohistan-Ladakh intraoceanic island arc and in the timing of exhumation of the Indian plate. In the west, a tectonic wedge consisting of the Kohistan-Ladakh intraoceanic island arc, ophiolitic mélange, and thrust slices of Lesser Himalayan and Tethyan correlatives of the Indian plate were in position and thrust over the Indian plate foreland prior to 47 Ma. Thereafter, Indian plate Lesser-, Greater-, and Tethyan Himalayan correlatives were exhumed from beneath the wedge (DiPietro et al., 2008), predominantly during the Paleogene with a pulse of deformation also in the earliest Miocene, at ca. 20 Ma (Argles et al., 2003, and references therein; DiPietro et al., 2021). Substantial rapid exhumation of the Indian plate hinterland is not recorded after this time, except in the Nanga Parbat region (Fig. 1C), a syntaxis of Lesser, Greater, and Tethyan Himalayan lithological correlatives, where rapidly accelerating exhumation is recorded over the Pliocene (e.g., Schneider et al., 2001). Thrusting and exhumation propagated southward toward the foreland in the mid- or late Miocene, and continued into the Pliocene (Burbank and Tahirkheli, 1985; Yeats and Hussain, 1987).

To the north of the Indian plate, moderate exhumation is recorded from Eocene times in the Kohistan island arc (van der Beek et al., 2009), yet the Karakoram terrane of the Asian plate records periods of rapid exhumation around 35–27 Ma, 17–13 Ma, 8–7 Ma, and 7.4–3.3 Ma (Dunlap et al., 1998; Wallis et al., 2016; Zhuang et al., 2018).

2.2. Foreland Basin Geology

In Pakistan, current basin environments along which the modern Indus River flows consist of: (1) the peripheral foreland basin that strikes east–west along the southern margin of the orogen and (2) the north–south-striking Lower Indus axial foreland basin along which the Lower Indus River debouches into its delta in the Arabian Sea (Fig. 1A).

2.2.1. Peripheral Foreland Basin

Foreland basin stratigraphy is, for the most part, invariant along strike in the orogen, with local minor facies variation, although formation names differ. In Pakistan, the Paleogene has a number of formation names for equivalent units in different areas (Pivnik and Wells, 1996). We adopt the formation names in our area of study, which for our Paleogene samples is the Hazara-Kashmir syntaxis (Hazara-Kashmir syntaxis; Figs. 1A and 1B), and the stratigraphy is recorded in Table 1. At this location, the Paleocene Lockhart Limestone is overlain successively by the latest Paleocene (57–55 Ma) Patala Formation, the early Eocene (55–53 Ma) Margala Hill and Chorgali formations, and the early–mid-Eocene (53–43 Ma) Kuldana Formation (Baig and Munir, 2007; Bossart and Ottiger, 1989; Ding et al., 2016b; Qasim et al., 2018). These formations, which stretch from marine facies to the transitional Kuldana Formation, are separated from the overlying continental alluvial facies by a late Eocene–Oligocene unconformity. Above the unconformity, there is the Murree Formation, also called the Balakot Formation in the Hazara-Kashmir syntaxis. In this syntaxis, the Murree Formation has a latest Oligocene maximum depositional age (MDA) as determined by the two youngest zircons within error, with a weighted mean U-Pb age of 22.6 ± 1.0 Ma (this study, section 4.2) from a sample collected near Paras, north of Balakot (Fig. 1B), which is supported by a grain dated at 22.7 ± 0.4 Ma (Ding et al., 2016b) from a section 15 km south at Muzaffarabad (Fig. 1B). Southwest of the Hazara-Kashmir syntaxis, at Murree Hill station (Fig. 1B), detrital mica Ar-Ar ages indicate an MDA younger than 24 Ma (this study, section 4.3). These MDAs agree with the early Miocene dating of the Murree Formation to the south, based on mammal fossils (Shah, 2009). Farther south, in the Kohat and Potwar plateaus (Fig. 1A), are the alluvial Kamlial Formation and overlying Siwalik Group, which are subdivided into the Chinji, Nagri, and Dhok Pathan formations (see Table 1 for stratigraphy). These formations are dated by magnetostratigraphy (Johnson et al., 1985) at 18–14 Ma, 14–11 Ma, 11–8.5 Ma, and younger than 8.5 Ma, respectively.

2.2.2. Lower Indus Axial Basin

The stratigraphy of the Lower Indus Basin in the Sulaiman and Kirthar regions is broadly correlative (Shah, 2009). It encompasses the early Eocene Ghazij Formation, the middle–late Eocene Kirthar Group, the Oligocene–early Miocene Chitarwata Formation, the late early–middle Miocene Vihowa Formation, and the middle Miocene–Pliocene rocks of the Siwalik Group (Roddaz et al., 2011; Shah, 2009; Zhuang et al., 2015), as denoted in Table 1. Facies are predominantly marine until the Chitarwata Formation, which transitions up from deltaic to fluvial facies. Fluvial facies then persist until the top of the section.

2.3. Paleodrainage Models

2.3.1. The Early Drainage Configuration of the Paleo-Indus: Evidence from the Indus Fan Sedimentary Archive

The oldest eastern Indus Fan sample (Integrated Ocean Drilling Program [IODP] 355, IODP U1456, and IODP U1457, Fig. 1A) to have been subject to detrital zircon U-Pb analyses is 15 Ma. This shows evidence of input from the Karakoram (Zhou et al., 2022), which indicates that the drainage basin of the paleo-Indus stretched as far back as the Shyok Suture Zone by this time (Fig. 1C). The oldest sample subjected to detrital zircon U-Pb dating in the western part of the Indus Fan (ODP 731; Fig. 1A) is ca. 30 Ma. This sample shows evidence of input from the Kohistan-Ladakh intraoceanic island arc/Asian plate (undifferentiated), which indicates that the river stretched back at least beyond the Indus Suture Zone (Fig. 1C) by that time (Feng et al., 2021). Likewise, mid-Eocene Owen Ridge sediments from Deep Sea Drilling Project (DSDP) 224 (Fig. 1A), considered to be early Indus Fan deposits (Clift et al., 2001a, 2002a), show bulk-rock ε_{Nd} signatures and K-feldspars with Pb isotopic compositions indicative of derivation from north of the Indian plate (Clift et al., 2001a). This indicates that the river's drainage basin stretched back at least as far as the Indus Suture Zone and Kohistan-Ladakh intraoceanic island arc at this time.

2.3.2. The Early Drainage Configuration of the Upper Axial Paleo-Indus: Evidence from the Indus Suture Zone Molasse

Clift et al. (2001b) considered that various isotopic provenance datasets and paleocurrents in Indus Suture Zone sedimentary rocks of early Eocene age indicate a contribution from the Lhasa terrane to the east, requiring along-strike, east-to-west flow along the suture zone at that time. However, Najman (2006) argued that an alternative source with a suitable signature could potentially be the Karakoram, located north of the suture zone sediments under discussion, and therefore along-strike transport and axial flow were not required. Sinclair and Jaffey (2001)

considered that their facies analyses of the suture zone sediments indicated internal rather than through-flowing drainage until at least the early Miocene. Later, Henderson et al. (2010) reported that the oldest suture zone sedimentary rocks to contain both micas derived from the Indian plate and zircons derived from the Asian plate is dated at younger than 23 Ma. From these mixed-source sedimentary rocks and the accompanying facies analysis, they considered that the Indus River was flowing in the suture zone at that time. However, it should be noted that: (1) micas were also recorded in older suture zone sedimentary rocks, but they were of too small a grain size to analyze; (2) Indian plate material with low muscovite fertility, such as from the Tethyan Himalaya, may well have contributed to the suture zone rocks earlier; and (3) an open question remains as to why the first appearance of micas interpreted as Indian-derived was not also accompanied by an influx of Paleozoic and older zircons, which are also typical of the Indian plate. While subsequently, such old zircons, interpreted as Indian rather than Asian-derived, have been documented in suture zone sediments as old as ca. 50 Ma (Bhattacharya et al., 2021), they are, nevertheless, not present in the samples analyzed for white mica Ar-Ar analyses by Henderson et al. (2010). While mineral sorting due to different hydraulic regimes of zircon versus mica (Malusà et al., 2016) could explain the difference, we suggest that—with the benefit of subsequent better characterization of the ages of micas from the southern margin of the Asian plate (Zhuang et al., 2018)—an Asian Karakoram provenance may provide an alternative provenance for these micas. Regardless, mixed Indian-Asian provenance, unaccompanied by facies data indicating deposition in a major river, does not indicate east–west through-flow of drainage. Bhattacharya et al. (2021) demonstrated from provenance data that detritus from the east was transported westward by ca. 27 Ma. Thus, we may conclude that an axial Upper Indus flowed westward by Oligocene times. Prior to that, the suture zone was a depocenter, but it may have been externally or internally drained.

2.3.3. Early Drainage Configuration of the Upper Transverse Paleo-Indus River: Evidence from the Peripheral Foreland Basin Deposits

In the peripheral foreland basin, detrital blue-green hornblende considered to be derived from the Kohistan-Ladakh intraoceanic island arc is first recorded in the Kohat and Potwar plateaus from 11 Ma (Nagri Formation) and interpreted as paleo-Indus deposits (Abbasi and Friend, 1989; Cerveny et al., 1989). Ullah et al. (2015)

applied geochemistry and petrography to the Chinji Formation (14–11 Ma) to record material from the Kohistan-Ladakh intraoceanic island arc and Indus Suture Zone. Based on petrography, Najman et al. (2003) recorded arc-derived detritus in the Potwar Plateau at 18 Ma, which is the start of the section they studied, from which they interpreted that this time represents the first arrival of sediment from the Upper Indus River to the foreland basin in this region. Still, later work (Ding et al., 2016b; Qasim et al., 2018) recorded arc-derived zircons in the foreland basin latest Paleocene to early Eocene Margala Hill and uppermost Patala formations, which indicates derivation from north of the Indus Suture Zone/Main Mantle Thrust since at least 55 Ma.

While the above provenance data indicate derivation from material as far north as the Kohistan-Ladakh intraoceanic island arc since Eocene times, whether these rocks represent the deposits of the paleo-Indus is debated (Cerveny et al., 1989; Willis, 1993; Zaleha, 1997). Chirouze et al. (2015) proposed a Lhasa terrane origin for detrital zircons with old fission-track ages in the Chinji Formation. This would indicate that the contributing drainage basin stretched into the Shyok Suture Zone and Asian plate by this time and was therefore likely the paleo-Indus. However, we suggest that such grains may also be derived from the Indian Himalayan units south of the Kohistan-Ladakh intraoceanic island arc, as can be argued due to their occurrence in the Siwalik foreland basin sedimentary rocks of Nepal, which were deposited by rivers that did not stretch back to Asia (Bernet et al., 2006).

However, more definitive evidence of deposition from the paleo-Indus comes from detrital mica Ar-Ar data. Lag times of detrital mica Ar-Ar ages from Kamlial Formation Potwar Plateau sedimentary rocks indicate rapid exhumation of the upland source region from 16 Ma to 14 Ma (Najman et al., 2003). The exhuming source area was interpreted by those authors to be the Karakoram and/or Nanga Parbat region, which is consistent with two sets of bedrock data from those regions (Treloar et al., 2000; Zhuang et al., 2018, and references therein). Due to their locations, the derivation of micas from either location strongly suggests transport by a paleo-Indus. Furthermore, detritus delivered by possibly ancient smaller tributaries draining only the Indian plate and arc would have had a distinct and different signature, with a higher proportion of Indian plate detritus, for example, the mid-Miocene Kamlial Formation sample CP96-6A from Najman et al. (2003), and presumably those samples from the Eocene Kuldana Formation with a high proportion of old zircons at Muzaffarabad (Ding et al., 2016b; see section 5.2 for further discussion).

2.3.4. Evolution of the Lower Indus Paleodrainage

Within the basin, the position of the Ganges-Indus drainage divide over time has long been debated, with various authors proposing that parts of the current Gangetic catchment used to flow into the Indus Fan (e.g., DeCelles et al., 1998), and the current Indus River catchment flowed into the Bengal Fan (e.g., Burbank et al., 1996) at various times. Clift and Blusztajn (2005) noted a change to more negative ε_{Nd} values in the Indus Fan at 5 Ma, which they interpreted as the drainage diversion of the major Indian plate-draining Punjabi Indus River tributary system of the Jhelum, Chenab, Ravi, and Sutlej rivers (Figs. 1A and 1C) from a previous routing toward the Ganges and the Bengal Fan to the east.

However, the above argument was countered by Chirouze et al. (2015), who looked at both spatial and temporal trends at the range front and Indus Fan. They considered that the change in the signal was due to differential exhumation in the hinterland rather than drainage reorganization. They compared ε_{Nd} data between the range front and Indus Fan for both the present day and the Miocene (using Chinji Formation foreland basin data for the Miocene range front). They recorded a spatial variation of four ε_{Nd} units between the range front and the Indus Fan for both mid–late Miocene times and modern day (Miocene range front and Indus Fan values were −6 and −10, respectively; modern-day range front and Indus Fan values were −10 and −14, respectively. This suggests a stable drainage pattern for the Lower Indus since at least the mid–late Miocene. From the data above, they noted a negative shift of ∼3 ε_{Nd} units between the Miocene and the modern day at the range front (comparison of Miocene foreland basin sedimentary rocks with modern-day Upper Indus values) and a similar shift in the Indus Fan. From this temporal shift they therefore concluded that the variation over time was due to the changing exhumation rates of the contributing source regions, with the exhumation and thus contribution of the Karakoram/Indian plate syntaxial Himalaya increasing at the expense of the more positive Kohistan-Ladakh intraoceanic island arc (Table 1) explaining the shift in ε_{Nd} values in the Indus Fan at 5 Ma. They supported their proposal of variations in exhumation using detrital zircon fission-track (ZFT) data, interpreting a decrease in older ZFT ages after 12 Ma as due to decreased input from the Kohistan-Ladakh intraoceanic island arc. Later, the original proponents of the drainage-capture hypothesis (Clift and Blusztajn, 2005) concurred with the view of Chirouze et al. (2015) that changes in the tectonics of the hinterland were the more likely cause of the geochemical

change in the Indus Fan at 6 Ma (Clift et al., 2019; Zhou et al., 2022). Thus, exactly when the Punjabi tributary system joined the Indus trunk river remains unknown. This question, namely the evolution of the downstream Indus, is the focus of this paper.

The location of where the Indus River exited to the ocean in the past retains a level of uncertainty. Today, the Indus River debouches to the Arabian Sea to the south of the Lower Indus Axial Basin. These deposits are recorded in the eastern Sulaiman and Kirthar regions of the Lower Indus Axial Basin (Welcomme et al., 2001; Fig. 1A). Zhuang et al. (2015) showed that zircons from the Kohistan-Ladakh intraoceanic island arc are recorded in these sediments from at least early Oligocene times; they considered that detrital zircon U-Pb data indicate input from the Karakoram from at least mid-Miocene times, and that Sr-Nd data indicate a paleo-Indus origin from 50 Ma. Roddaz et al. (2011) carried out mixture modeling on their Sr-Nd data and concluded that there was an appreciable input from the Karakoram since 50 Ma.

However, Paleogene deltaic facies have also been identified in the Katawaz remnant oceanic basin (Fig. 1A) to the west (Qayyum et al., 2001). In view of the differing compositions and provenance of these two deltaic systems, Roddaz et al. (2011) proposed two river delta–fan systems, with the Katawaz system debouching into the Khojak submarine fan, and the sediments of the Lower Indus Axial Basin debouching into the Indus Fan. Provenance data from the Katawaz rocks show that that the drainage basin stretched back at least as far as the Kohistan-Ladakh intraoceanic island arc by Miocene times (Carter et al., 2010), with a paucity of data currently precluding earlier documentation. For a full evaluation of the Indus River delta–fan system and the spatial evolution, more data are needed from the Katawaz basin; data presented in this paper provide a direct comparison of peripheral foreland basin records and terminal sinks in the delta and ocean.

3. METHODS

3.1. Rationale and Approach

To determine when the Punjabi tributary system joined the Indus trunk river, we leverage the fact that the tributaries have a very different drainage basin lithology than the Indus trunk river; the former includes only Himalayan units, while the drainage basin of the latter also includes the Kohistan-Ladakh intraoceanic island arc and Asian plate (Fig. 1C), which have very different isotopic and geochemical signatures than the Indian plate (Table 1). This difference is clearly reflected in both the Sm-Nd and zircon U-Pb characteristics of the Indus trunk river versus the Punjabi tributary system: Figures 2 and 3A (inset) show that, compared to the modern Indus trunk river, the Punjabi tributaries have a more negative ε_{Nd} value and a much lower proportion of young arc-aged grains (Alizai et al., 2011; Chirouze et al., 2015), a signature that extends back into the ancient sedimentary record (Exnicios et al., 2022; Najman et al., 2009).

We took a similar approach to Chirouze et al. (2015) in hypothesizing that prior to the Punjabi tributary system joining the Indus river, the sedimentary repositories upstream and downstream of the confluence should look similar in terms of provenance. After the tributary system joined the Indus River, the repository upstream of the confluence should have remained similar (unless synchronously affected by a tectonic-induced change in the hinterland), but the downstream repository should show increased input from Himalayan Indian plate units.

Therefore, we compared data upstream (our new foreland basin data) and published data
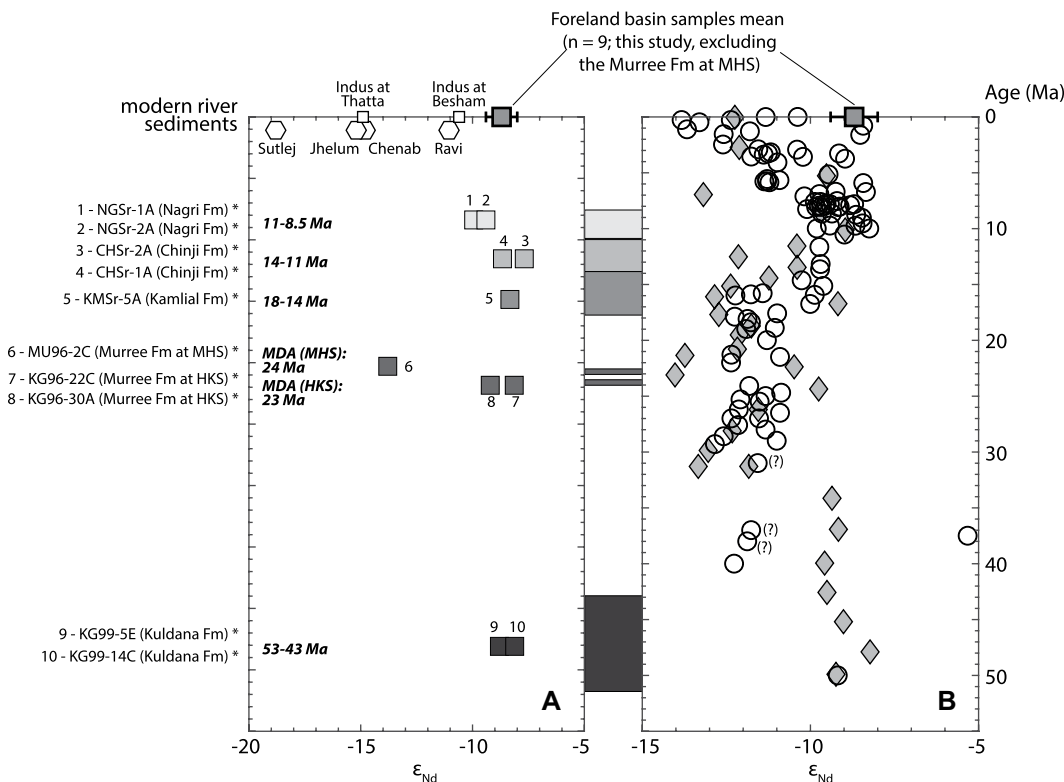
Figure 2. ε_{Nd} **values from the upstream peripheral foreland basin in (A) Pakistan and downstream Lower Indus Axial Basin and (B) the Indus Fan through time. In panel A, numbers by squares refer to sample numbers at left. Asterisks indicate new data. White squares indicate data from the modern Indus River at Besham and Thatta; hexagons indicate data from the modern Punjabi tributaries (Clift et al., 2002b; Alizai et al., 2011; Chirouze et al., 2015). In panel B, diamonds indicate data from the Sulaiman and Kirthar regions of the Lower Indus Axial Basin (Roddaz et al., 2011; Zhuang et al., 2015); circles indicate data from the Indus Fan (Clift et al., 2001a, 2019; Clift and Blusztajn, 2005; Zhou et al., 2021; Feng et al., 2021). Question marks next to three mid-Eocene samples represent uncertainties in the ages of** those samples, as depicted in the original publication of Clift et al. (2001a). HKS—Hazara-Kashmir syntaxis; MHS—Murree Hill station; MDA—maximum depositional age as determined from detrital grain ages (see sections 2.2.1, 4.2, and 4.3 in the text). Grey horizontal shading between plots A and B denotes roughly equivalent time periods.
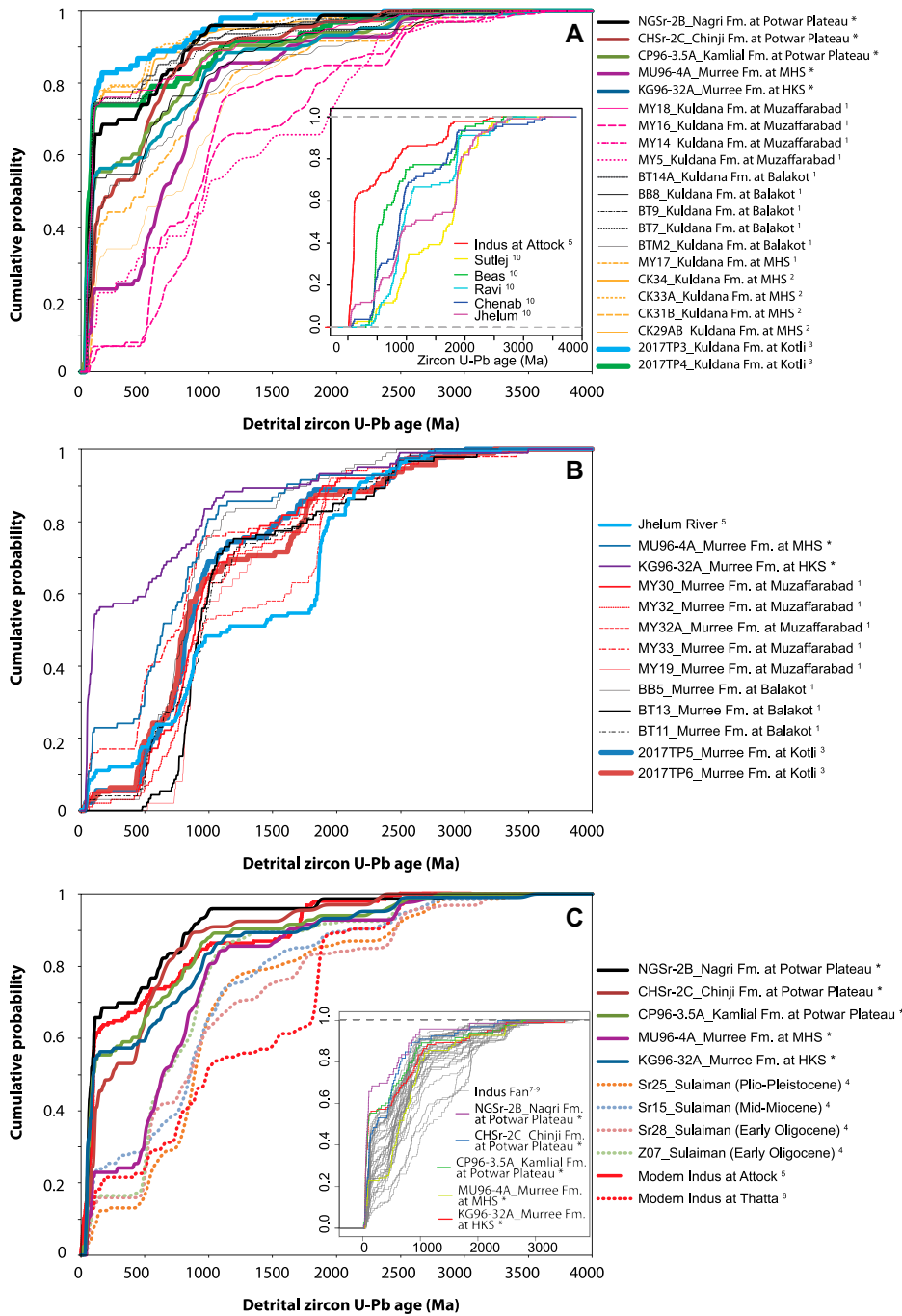
Figure 3. Detrital zircon U-Pb data shown as cumulative age distribution plots. (A) Data for the Pakistan peripheral foreland basin, excluding data for the Murree Formation except for our new data. Kuldana Formation samples are early–mid-Eocene, Murree Formation samples are early Miocene, Kamlial Formation sample is early–mid-Miocene, Chinji Formation sample is mid-Miocene, and Nagri Formation sample is late Miocene (Table 1). (A, inset) Modern river data comparing the Indus at the range front at Attock with rivers of the Punjabi tributary system. (B) All Murree Formation data, both new and published, with comparison to the Jhelum modern river data. Murree Formation is early Miocene. (C) Comparison of data from the peripheral foreland basin, downstream Lower Indus Axial Basin, and (C, inset) Indus Fan. Eocene peripheral foreland basin data are omitted from the figure as there are no comparative data from the downstream repositories. HKS—Hazara-Kashmir syntaxis; MHS—Murree Hill station. All new data are asterisked. Samples with superscripts are published data, as follows: 1—Ding et al. (2016b); 2—Qasim et al. (2018); 3—Awais et al. (2021); 4—Zhuang et al. (2015); 5—Clift et al. (2022); 6—Clift et al. (2004); 7—Clift et al. (2019); 8—Zhou et al. (2021); 9—Feng et al. (2021); 10—Alizai et al. (2011).

Miocene study of the Pakistani peripheral foreland basin to now include foreland basin rocks from the Eocene to late Miocene. This allows a more complete assessment of the evolution of the Lower Indus to be determined. Secondly, we incorporate not only ε_{Nd} data from mudstones, but also new and previously published zircon U-Pb data to assess provenance, and mica $^{40}Ar/^{39}Ar$ data to assess exhumation. Therefore, in addition to using both onshore and offshore repositories to limit the potential effects of fertility, diagenetic, and hydraulic sorting biases, our multi-proxy approach provides additional mitigation, since: (1) zircons are resistant to diagenesis, (2) we assessed evidence from both the mud and sand-grain size fractions with the use of both bulk- and single-grain approaches, and (3) we obtained data from both zircon and mica grains that respond differently to the hydraulic regime (e.g., Garzanti and Andò, 2019; Garzanti et al., 2009; Malusà et al., 2016). Furthermore, since white mica is rare in the Kohistan-Ladakh intraoceanic island arc, exhumation patterns of the Karakoram and Indian plate Himalaya can be considered in isolation using this tech-

downstream from the Punjabi tributary system. Previous work used the Indus Fan as the downstream comparative repository. We used both the deltaic record in the Sulaiman and Kirthar region, and the Indus Fan archive, since onshore sedimentary archives are typically more prone to diagenetic alteration than marine records, while distal deposits are more prone to the effects of hydraulic sorting (e.g., Garzanti et al., 2020) and contain evidence of subordinate extraneous (non-Indus River) sources to the Himalayan orogen, such as the Deccan Traps of peninsular

India input to the Indus Fan (Clift et al., 2019; Garzanti et al., 2020; Yu et al., 2019). The Indus Fan record is a composite repository of material recovered from the Owen Ridge and Western Fan from DSDP 224 (Eocene–Miocene) and ODP 720, 722, and 731 (Eocene–Pleistocene) sites, and IODP 355 sites U1456 and U1457 in the Eastern Fan (Neogene only; Clift et al., 2019; Feng et al., 2021; Zhou et al., 2022; Fig. 1A).

Our dataset builds on the previous work of Chirouze et al. (2015) in two ways. Firstly, it expands the time range from the previous mid-

nique, because it is unbiased by potential issues related to dilution and fertility.

3.2. Samples and Analyses

3.2.1. Samples

We analyzed five sandstones for detrital zircon, 10 mudstones for Sr-Nd isotopes, and three sandstones for mica ^{40}Ar/^{39}Ar. The samples analyzed (Figs. 1A and 1B) are from the Kuldana Formation in the Hazara-Kashmir syntaxis at Paras north of Balakot, the Murree Formation in both the Hazara-Kashmir syntaxis and at Murree Hill station, and the Kamlial, Chinji, and Nagri formations of the Chinji section of the Potwar Plateau, the latter being the same location from which Chirouze et al. (2015) took their samples. A summary of our sample information is tabulated in Table S1 in the Supplemental Material[1]. Our samples from the Kuldana Formation are structurally imbricated within the Murree Formation (Najman et al., 2002). Originally, Najman et al. (2002) considered these structural imbrications to be from the Patala Formation, based on the work of Bossart and Ottiger (1989), who did not recognize the Kuldana Formation. However, more recent detailed mapping (Ding et al., 2016b) and the better agreement of biostratigraphic ages from the structural imbricates (early–mid-Eocene; Bossart and Ottiger, 1989) of the Kuldana Formation rather than the Patala Formation (section 2.2.1) suggests reassignment of these imbricates from the Patala to Kuldana Formation.

3.2.2. Sr-Nd Bulk Analyses

Sr and Nd isotopic analyses of bulk mudstones were carried out at the Natural Environment Research Council Isotope Geosciences Laboratory, Keyworth, Nottingham, UK. Samples were leached in dilute acetic acid to remove carbonate material, and then dissolved using HF-HNO^3 and converted to chloride form. Sr and a bulk rare earth element (REE) fraction were separated using AG 50W × 8 cation columns, and Nd was separated from the bulk REE using LN-Spec columns. Sr and Nd were analyzed on a Thermo Scientific Triton thermal ionization mass spectrometer.

3.2.3. Zircon U-Pb Analyses

Detrital zircon U-Pb ages were acquired using laser ablation–inductively coupled plasma–mass spectrometry at the London Geochronology Centre, University College London, UK. To avoid bias, polished grain mounts were made, without hand picking, directly from Diiodomethane sink fractions with a grain size of ≤300 μm. Each laser spot (25 μm) was placed on the outermost parts of each grain to target the youngest growth stage. Between 150 and 320 grains were analyzed for each sample to provide statistical confidence of detecting all component ages. Data were processed using GLITTER version 4.4 data reduction software with age-standard bracketing to correct for mass fractionation. Between 8% and 15% of ages were rejected, due to high discordance from lead loss, zoning, or mixing of growth zones. One exception was the Chinji Formation, which contained an unusually high number (60%) of discordant grains. Most of these discordant grains are associated with ages of between 120 Ma and 75 Ma and consistent with lead loss, likely due to source weathering.

3.2.4. Muscovite Ar-Ar Analyses

Muscovite Ar-Ar ages were analyzed at the Argon Geochronology Laboratory at Vrije Universiteit Amsterdam, Netherlands. Individual grains ranging from 125 μm to 1000 μm were handpicked under a binocular microscope to avoid obvious weathering or inclusions. After irradiation at the Oregon State University TRIGA nuclear reactor, total fusion analyses were carried out with a Thermo Fisher Scientific HELIX MC Plus multicollector noble gas mass spectrometer, fitted with 10^{13} Ohm amplifiers. Data reduction was done using ArArCALC2.5 (Koppers, 2002).

Detailed methodologies are provided in Text S1, and results are reported in Tables S1 (Sr-Nd data), S2 (zircon U-Pb data), and S3 (mica Ar-Ar data).

4. RESULTS AND INTEGRATION WITH PUBLISHED DATA

4.1. Sr/Nd Bulk

Data are recorded and portrayed in Table S1 and Figures 2 and S1. There is little significant variation in ε$_{Nd}$ values from the Eocene Kuldana Formation to the late Miocene Nagri Formation, with values ranging between −7.0 and −9.2 (Fig. 2A). The exception to this overall similarity is the Murree Formation at Murree Hill station, with a value of −13.8. We note that previous work for the Chinji Formation records values of −3.8 to −7.7 (Chirouze et al., 2015). This difference could perhaps reflect the previous use of

sand for analysis instead of mud in the current research (see Jonell et al., 2018, for further discussion). There are no modern-day data available for the range front. The Upper Indus has a value of −10.8 at Besham (Clift et al., 2002b), which is located just downstream of the Kohistan arc (Figs. 1B and 1C), and we can extrapolate that values should be more negative than this at the range front, after the river has passed over the Greater and Lesser Himalaya. Values at the delta front at Thatta are −14.9 (Clift et al., 2002b).

We carried out mixture modeling on the foreland basin material (Fig. S1). The mixture modeling is complicated by the number of end-member contributors; today, sediment in the Upper Indus River contains material from the Lhasa terrane, Karakoram, Kohistan-Ladakh intraoceanic island arc, suture zone, and the Indian plate units of the Greater-, Lesser-, and Tethyan Himalayan correlatives. Overlapping signatures of some units (e.g., between the Karakoram and Tethyan Himalaya, and between the Kohistan-Ladakh intraoceanic island arc and ophiolitic mélange of the suture zone) also add uncertainty. We started with the premise that, from the zircon data, we are confident that the foreland basin contains material from the Kohistan-Ladakh intraoceanic island arc (section 4.2) from the oldest sediments studied, namely the early–mid-Eocene Kuldana Formation. Thus, the Kohistan-Ladakh intraoceanic island arc forms the apex of our model, and various mixture couplings are calculated with this apex and other potential end members. The modeling shows that all data can be explained by a mix of Indian plate and Kohistan-Ladakh intraoceanic island arc inputs, and contribution from the Karakoram and Lhasa terrane is equivocal. The Murree Formation sample from Murree Hill station requires considerable input from Greater Himalayan lithological correlatives.

The Sr-Nd compositions of the samples show trends that are consistent with simple mixing between mafic and more evolved sources. There is some scatter in the data toward high Sr^{87}/Sr^{86} values that may result from weathering or diagenesis. However, we are confident that the dominant trends reflect changes in provenance, as described above.

4.2. Detrital Zircon U-Pb Analyses

Data are recorded and portrayed in Table S2 and Figures 3, S2, and S3. We compiled our new data from the Murree Formation at Paras, north of Balakot in the Hazara-Kashmir syntaxis and at Murree Hill station (dated at younger than 24 Ma), and from the Kamlial (18–14 Ma), Chinji (14–11 Ma), and Nagri (11–8.5 Ma) formations in the Potwar Plateau, with previously published data from the Kuldana and Murree

Formation rocks at Balakot, Muzaffarabad, and Kotli in the Hazara-Kashmir syntaxis and at Murree Hill station (Awais et al., 2021; Ding et al., 2016a; Qasim et al., 2018) and modern river data collected at the Main Central Thrust-correlative (Khairabad Thrust) at the range front at Attock (Alizai et al., 2011; Clift et al., 2022; Fig. 1B). We keep our observations of comparisons broad and conservative in nature, since various approaches to mineral separation and data processing procedures by different labs can cause variations in proportions of populations. We begin our summary at the marine-to-continental transition (the Kuldana Formation, section 2.2.1). We focus on the 200–40 Ma "arc-aged" population characteristic of the Kohistan-Ladakh intraoceanic island arc and Karakoram, and the older grains typical of the Indian plate and Karakoram, with emphasis on the 2300–1500 Ma population typical of the Lesser Himalayan lithological correlatives and the 1250–300 Ma population typical of the Greater Himalayan lithological correlatives (section 2.1.1; Table 1).

With the exception of the Murree Formation (which we portray separately in Fig. 3B and discuss separately in section 5.2), the proportions of the 200–40 Ma "arc-aged" populations remain approaching or >50% throughout the Neogene to present day. There is much variation within the Eocene Kuldana Formation, and a number of samples also show a majority of the grains to be arc aged (Fig. 3A; Table 1). By contrast,

the Murree Formation has a very low proportion of grains in the 200–40 Ma range in all samples analyzed from Murree Hill station, Muzaffarabad, and Balakot, although not at Paras north of Balakot in the Hazara-Kashmir syntaxis (Figs. 1B, 3B, and S2). Instead, these Murree Formation samples from Murree Hill station, Muazaffarabad, and Balakot have a high proportion of grains with ages typical of the Greater Himalaya. In contrast to the modern-day river sample at Attock (Figs. 3C and 1B), there is no 2300–1500 Ma population typical of the Lesser Himalayan lithological correlatives in any of the formations.

4.3. Mica Ar-Ar

Data are recorded and portrayed in Table S3 and Figures 4 and S4. We integrated our new data from the Murree Formation at Murree Hill station and the Chinji and Nagri formations with previous data from the Murree Formation in the Hazara-Kashmir syntaxis at Paras north of Balakot (Najman et al., 2001) and the Kamlial Formation (Najman et al., 2003; Fig. S4). We note that the number of grains analyzed for the Murree Formation at Paras north of Balakot (n = 257) and the Kamlial Formation (n = 277) is considerably higher than for the Murree Formation at Murree Hill station, the Chinji and Nagri samples (n = 59, 94, and 43, respectively). Thus the Balakot and Kamlial Formation datasets are

likely to have more completely captured the full spectrum of age populations.

The youngest grain in the Murree Formation at Paras in the Hazara-Kashmir syntaxis is 24.6 ± 0.7 Ma, the weighted mean of the youngest two grains overlapping within error at two sigmas is 24.8 ± 1.4 Ma, and the youngest peak population is 37 Ma. Pre-Cenozoic ages extend to older than 1500 Ma. Farther south, the youngest grain in the Murree Formation at Murree Hill station is 23.7 ± 0.1 Ma, which also forms one of the two youngest grains overlapping within error at 2 sigmas (weighted mean age of 23.85 ± 0.12 Ma). The youngest peak population is 28–24 Ma. Pre-Cenozoic ages extend to ca. 450 Ma. The youngest grain from the Kamlial Formation is 14.5 ± 0.7 Ma, and the weighted mean of the youngest two grains within error at 2 sigmas is 15.00 ± 1.10 Ma. The youngest peak population is 18 Ma, and pre-Cenozoic ages extend to ca. 450 Ma. The lowest Chinji Formation sample (CP96-7A; Najman et al., 2003; dated at 13.9 Ma) has a youngest grain at 14.1 ± 0.7 Ma, and this also forms one of the two youngest grains within error at 2 sigmas (weighted mean age of 14.43 ± 0.81 Ma). Pre-Cenozoic grains extend to 400 Ma. Our new sample from the Chinji Formation has a youngest grain age of 16.74 ± 0.1 Ma, the weighted mean of the two youngest grains overlapping within error at 2 sigmas is 25.95 ± 0.10 Ma, the youngest peak
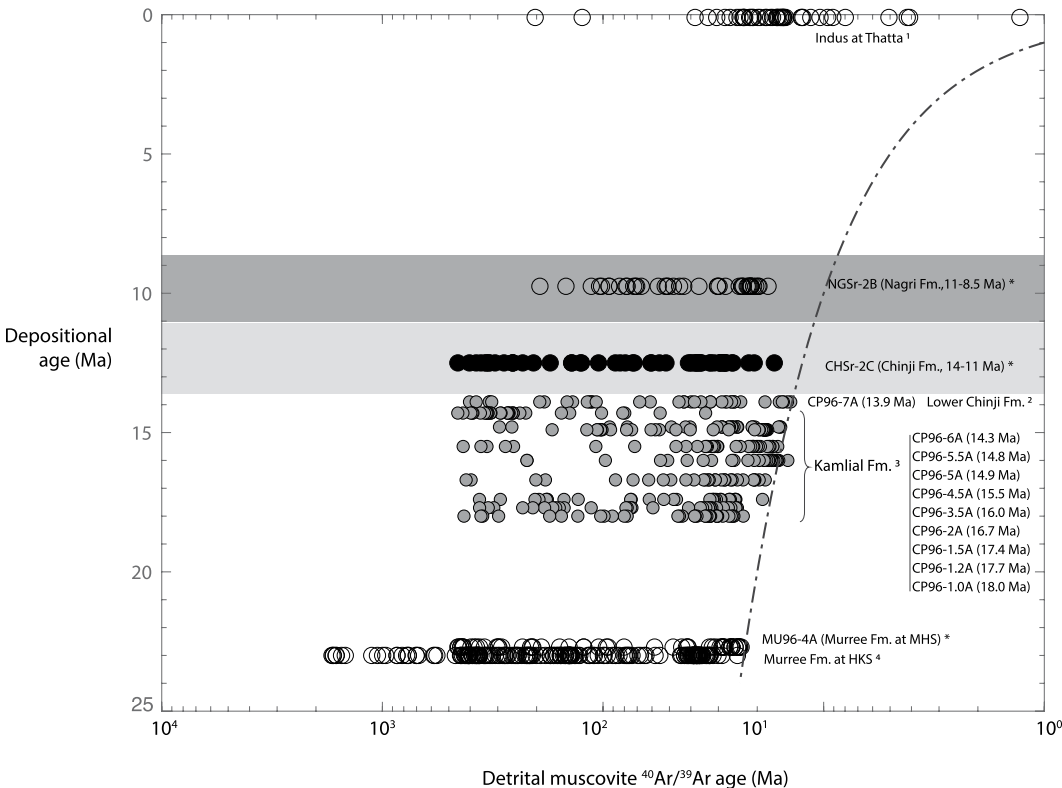
Figure 4. Ar-Ar mica data plotted against depositional age for new (asterisked) and published samples. Published data from: 1—Clift et al. (2004) for the modern Indus River data at Thatta; 2—Najman et al. (2003) for the lower Chinji Formation; 3—Najman et al. (2003) for the Kamlial Formation; 4—Najman et al. (2001) for the Murree Formation at the Hazara-Kashmir syntaxis. Apart from the lower Chinji Formation sample, Chinji Formation and Nagri Formation samples are not tied to the magnetostratigraphically dated section (Johnson et al., 1985; section 2.2.1 in the text), and therefore the depositional age range of these samples is shown by the gray bars. Note that Murree Formation samples are plotted on the *y*-axis at the age of their maximum depositional ages.

population is 29–28 Ma, and pre-Cenozoic ages extend to ca. 450 Ma. The youngest grain in the Nagri Formation is 17.9 ± 0.14 Ma, the weighted mean age of the two youngest two grains overlapping within error at 2 sigmas is 19.69 ± 0.12 Ma, the youngest peak population is 21 Ma, and pre-Cenozoic ages extend to ca. 200 Ma.

Good magnetostratigraphic age control for the Kamlial and lowest Chinji Formation allowed for periods of rapid hinterland exhumation to be determined from lag times. Rapid exhumation occurred in the hinterland between 16 Ma and 14 Ma (Najman et al., 2003; Fig. 4). The lack of independent depositional age constraints precludes calculation of lag times for the newly analyzed Murree, Chinji, and Nagri Formation samples. Up section from the Kamlial Formation, there is no evidence of grain ages approaching depositional age, until the modern river

sample at Thatta, although the number of grains analyzed is relatively small.

5. INTERPRETATIONS OF THE EVOLUTION OF THE LOWER INDUS DRAINAGE

5.1. When Did the Punjabi Tributary System Join the Paleo-Indus Trunk River?

As outlined in our rationale and approach (section 3.1), we determine when the Punjabi tributary system joined the main trunk river by comparing provenance data from upstream and downstream of the present-day confluence. We leverage the fact that unlike the paleo-Indus trunk river, the tributaries drain only the Indian plate terranes (Fig. 1C) and thus have a different provenance signature (section 3.1; inset of Figs. 2 and 3A).

As schematically presented in Figure 5, the following evidence should be met, at the time the tributary system joined the Indus trunk river:

(1) Prior to when the Punjabi tributary system joined the Indus catchment, the proportion of Indian plate detritus delivered to the Indus River should be comparable at the range front and at the river mouth, i.e., upstream and downstream of where the Punjabi tributary system now joins the modern Indus.

(2) After the Punjabi tributary system joined the Indus River, the proportion of Indian plate material in the Indus River downstream of the confluence with the Punjabi rivers should increase relative to the downstream's previous pre-reorganization proportion and be greater than coeval sediments upstream. However, the proportion of Indian plate material in the upstream should remain constant both before and after the proposed drainage reorganization.
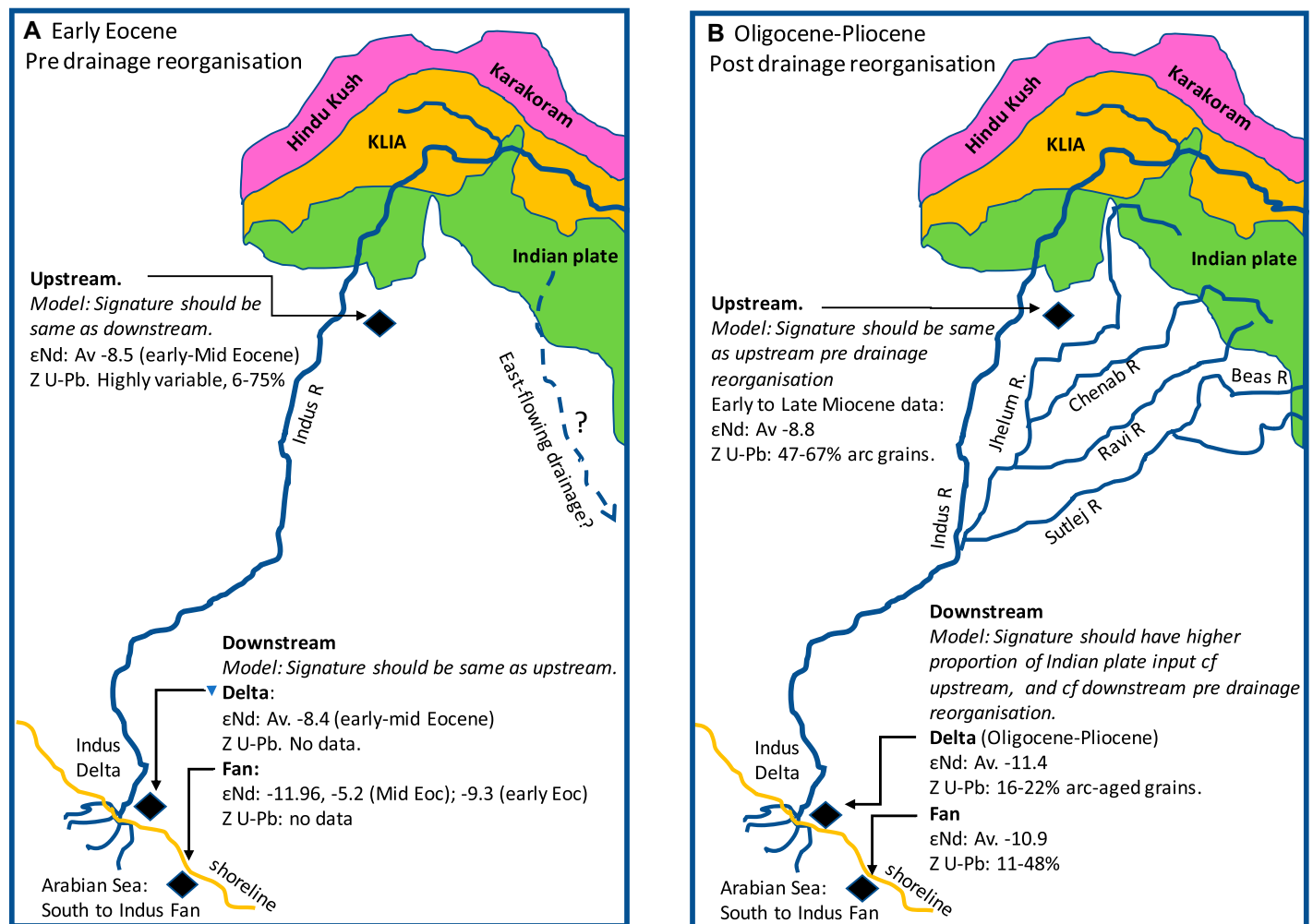

Figure 5. Schematic figure showing expected and actual changes in provenance characteristics of sedimentary archives upstream and downstream of the confluence, when the Punjabi tributary system joins the paleo-Indus trunk river, superimposed on the modern geology. More detail on analytical values summarized in this figure can be found in Table 1. Av—average; Eoc—Eocene; KLIA—Kohistan-Ladakh intraoceanic island arc; R—River; Z—zircon.

For the above predictions to be explored, the Indian plate, versus Karakoram, versus Kohistan-Ladakh intraoceanic island arc must be differentiable in the detritus of the foreland basin. Table 1 provides the typical zircon U-Pb and ε_{Nd} signatures of these units, alongside a summary of equivalent data from the peripheral foreland basin, and downstream in both the Sulaiman-Kirthar region and Indus Fan. The insets of Figures 2 and 3A show the difference between the modern Indus trunk river, which drains the Asian plate, arc, and Indian plate, versus the modern Punjabi tributary system, which primarily drains only the Indian plate.

For the interpretations made from this upstream–downstream comparison to be valid, the rocks at the locations evaluated must be the products of the paleo-Indus trunk river. While all three repositories studied—the peripheral foreland basin, the Lower Indus Axial Basin, and the Indus Fan—show evidence of derivation from at least as far north as the Kohistan-Ladakh intraoceanic island arc since Eocene times, we acknowledge that evidence for input from north of the Shyok Suture Zone can be equivocal (see sections 2.3.1, 2.3.3, and 2.3.4).

Below, we summarize the salient points regarding the upstream and downstream repositories that are relevant to the characteristics required to document the timing of conjoinment of the Punjabi tributary system with the Indus trunk river, as described above in this section. Separately, in section 5.2, we discuss the Murree Formation, which is anomalous at Murree Hill station, Muzzafarabad, and Balakot, but not at Paras.

5.1.1. Comparison of the Upstream Peripheral Foreland Basin Material with the Downstream Repositories in Terms of Sr-Nd Data

Our upstream data (peripheral foreland basin) show that values have remained broadly constant from the start of the early–mid-Eocene Kuldana Formation (Fig. 2A) until the late Miocene Nagri Formation, when values become a little more negative. $\varepsilon_{Nd}(0)$ values in the downstream repositories are similar to those upstream in the early Eocene. However, values in the downstream repositories become more negative than those upstream by mid-Eocene in the Indus Fan and around the Eocene–Oligocene boundary in the Lower Indus Axial Basin (Fig. 2B). This shift indicates a greater input of material from the Indian plate Himalayan terrane at this time.

From the more negative $\varepsilon_{Nd}(0)$ values recorded below the confluence compared to above it throughout the Neogene, we interpret that the Punjabi tributary system has drained into

the paleo-Indus trunk river throughout the Neogene, and that the present drainage configuration was therefore established during the Paleogene.

The consistency of ε_{Nd} values from the Eocene to the Neogene in the upstream repository, in contrast to the shift to more negative values in the downstream repositories, should reflect the time when the Punjabi tributary system joined the Indus trunk river. However, the difference in the time of the downstream shift, which took place at the Eocene–Oligocene boundary in the Lower Indus Axial Basin delta deposits and in the mid-Eocene in the Indus Fan, indicates that more research is required before we can pinpoint exactly when the tributary system joined the Indus river. Nevertheless, with available data we can conclude that the tributaries joined the Indus river at or before the start of the Oligocene (Fig. 5).

5.1.2. Comparison of the Upstream Peripheral Foreland Basin Material with the Downstream Repositories in Terms of Detrital Zircon U-Pb Data

Although intraformational variability, lack of data from the Oligocene in the peripheral foreland basin, and lack of data from the Eocene in the downstream repositories limits the comparison, the data are consistent with the interpretations determined by the Sm-Nd data, that the Punjabi tributary system joined the Indus trunk river by Oligocene times (section 5.1.1; Fig. 5). The proportion of 200–40 Ma arc-aged grains remains high throughout the Miocene in the peripheral foreland basin, and these values are higher than the Oligocene–Pliocene values in both downstream repositories (Figs. 3A and 3C; Table 1). Data from the Eocene peripheral foreland basin are highly variable. However, at least some samples have a proportion of arc-aged grains that is similar to the proportions of the Neogene peripheral foreland basin, which is consistent with the pattern shown in the Sm-Nd data.

Figure S3 illustrates the river's evolution well, particularly in comparison to the Lower Indus Axial Basin. Downstream samples have a greater affinity to Indian plate rocks and the modern Indus at its mouth at Thatta, compared to the upstream peripheral foreland basin rocks, which have greater affinity to the arc and Asian plate, and the modern-day Indus at the range front at Attock.

The variation in zircon U-Pb age spectra and ε_{Nd} values between the onshore and offshore downstream paleo-Indus and the eastern and western Indus Fan (Figs. S1 and S3) is intriguing. These variations could be the result of a number of factors: differences in sample preparation procedures between operators, the down-

stream influence of hydraulics, or the contribution of additional material downstream.

5.2. Interpretation of the Murree Formation

Compared to the other peripheral foreland basin sediments sampled, the zircon U-Pb data show significantly higher proportions of old grains in the Murree Formation at Murree Hill station, Kotli, and at Balakot and Muzaffarabad in the Hazara-Kashmir syntaxis, but not at Paras north of Balakot (Figs. 3B and S2; Table 1). Where accompanying Sr-Nd data are available (Murree Hill station and Paras only), there is a corresponding change to more negative ε_{Nd} values at Murree Hill station (Fig. 2A), which mirrors the change noted in the zircon data. This signature indicates a higher proportion of material derived from the Indian plate (also see Fig. S3). These deposits may be interpreted as the paleo-Jhelum Punjabi tributary, which has a zircon U-Pb spectrum similar to that of the Murree Formation (Fig. 3B), and a drainage basin consisting predominantly of the Indian plate (Fig. 1C). The spatial distribution of the samples we analyzed is consistent with this interpretation: a Himalayan-derived, paleo-Jhelum–type signature is prevalent in Murree Formation samples at Muzaffarabad (Fig. 1B), which is located on the modern-day Jhelum River, at Murree Hill station, which is downstream and ∼10 miles to the west of the modern Jhelum River, and at Kotli, which is downstream and 20 km east of the modern Jhelum River. It is also prevalent at Balakot, ∼15 miles upstream of the modern Jhelum River, which we suggest could have been in the flood plain of the paleo-Jhelum. Five miles farther north, near Paras, the signature is more arc-like and in this paleodrainage scenario, we propose lies outwith the floodplain of the paleo-Jhelum. We note that only at Muzaffarabad, through which the modern Jhelum River flows, a paleo-Jhelum–type signature is also recorded, in some samples, in the underlying Eocene Kuldana Formation. This may reflect the early initiation of this river, which was not large enough in its early evolution to affect the downstream.

Alternatively, the anomalous signature from the Murree Formation compared to the rest of the Cenozoic sediments in the peripheral foreland basin may reflect increased input from the Himalaya attributable to a pulse of exhumation recorded in the Himalaya in the early Miocene (section 2.1.2). A coeval change to greater input from the Indian plate is also recorded in the Indus Fan (Feng et al., 2021) and Kirthar ranges (Zhuang et al., 2015), which supports

this interpretation. Further analyses from Murree Formation samples distal to the Jhelum River should distinguish between these two alternative hypotheses.

The difference in Murree signature compared to the rest of the foreland basin cannot be ascribed to bias associated with grain-size variation, since the difference is reflected in both bulk-rock Sr-Nd and zircon proxies. Nor is there any reason to consider that a potential difference in the degree of diagenesis caused the difference, since zircons are largely unaffected by this process.

5.3. What Caused the Change in the Geochemical Signature of the Indus Fan at 6–5 Ma?

The more recently proposed alternatives to drainage reorganization (Clift and Blusztajn, 2005) to explain the geochemical shift in the Indus Fan at 6–5 Ma all involve tectonic explanations, namely variations in exhumation of the hinterland terranes, although the extent to which increased exhumation of the Lesser Himalaya versus Greater Himalaya versus Karakoram is responsible is debated (Chirouze et al., 2015; Clift et al., 2019; Zhou et al., 2022). Changes in monsoonal intensification are not considered to have been a major influence (Clift et al., 2019; Zhou et al., 2022).

To what extent do our data support a tectonic explanation? We focus on the peripheral foreland, which should provide the most tectonically influenced archive, above any downstream influence from the Punjabi tributary system. We compare our data from the Nagri Formation (11–8.5 Ma; Table 1) to modern-day Indus data at the range front, as this time period encompasses the 6–5 Ma date over which the geochemical shift in the Indus Fan occurred.

The average ε_{Nd} value of the two samples from the Nagri Formation is −9.65. No data are available for the modern Indus at the range front. The spatially closest sample is from Besham, just south of the Main Central Thrust (Fig. 1C). This sample has a value of −10.7, and we would expect a more negative value by the time the river had crossed to the range front, having flowed over more of the Greater Himalaya and most negative Lesser Himalaya (Table 1). Thus, the shift to more negative ε_{Nd} values between the Nagri Formation and the estimated value for the range front in modern times shows that variation in upland tectonics over this time period could have resulted in the shift to more negative ε_{Nd} values seen in the Indus Fan over this time period.

Assigning zircon U-Pb age populations to distinct provenances is challenging with respect to

overlap of the older Karakoram and Indian plate grains. Nevertheless, the 2300–1500 Ma population is typical of the Lesser Himalaya. This population makes up 3% of the Nagri sample. There is no sample from the modern Indus River at the range front. However, there is a sample from upstream at Attock (Fig. 1C). This sample has an 11% contribution from the 2300–1500 Ma population, and we would predict a higher proportion of that population after the river flowed over a greater proportion of Indian plate material. the shift to a higher proportion of zircons with ages indicative of Lesser Himalayan input between the Nagri Formation and the modern day (Fig. 3) therefore supports our observations from the Sm-Nd data that upstream variations in tectonics could have resulted in the geochemical shift in the Indus Fan.

There are no modern river mica $^{40}Ar/^{39}Ar$ data from the range front. Modern river $^{40}Ar/^{39}Ar$ mica data from the Indus trunk river at its mouth at Thatta show Plio-Pleistocene grains (5–1 Ma) that are indicative of rapid exhumation (Clift et al., 2004). Recording of these young grains in the trunk river but not in the tributaries draining only the Indian plate or Indian plate plus Hindu Kush (Clift et al., 2004; Najman et al., 2009; Zhuang et al., 2018) is consistent with the viewpoints of, for example, Chirouze et al. (2015) and Clift et al. (2022), that the Karakoram and/or the Nanga Parbat syntaxis supplied this young material. Lag times determined from mica data from the Neogene peripheral foreland basin sedimentary rocks show no clear indication of rapid exhumation of the micas' source region after 16–14 Ma (Fig. 4), although the n-values are small, and populations may have been missed. Therefore, a period of rapid exhumation occurred sometime between Nagri Formation times and present day, which is consistent with the view that changing exhumation in the hinterland was responsible for the geochemical shift at 5 Ma in the Indus Fan.

6. CONCLUSIONS

When the Lower Indus River broadly attained its current drainage configuration, in particular when the Punjabi tributary system joined the main trunk river, is undocumented. Comparison of ε_{Nd} bulk-rock data and detrital zircon U-Pb data from Cenozoic paleo-Indus sedimentary rocks both upstream and downstream of the confluence of the Indus with the Punjabi tributary system shows that throughout the Neogene, greater proportions of Indian plate material are recorded in the downstream compared to the upstream repositories. Therefore, we conclude that the Punjabi tributary system, which transports predominantly Indian

plate detritus, had joined the Indus trunk river prior to the Neogene.

While provenance indicators show that the proportion of Indian plate material remained constant from the Eocene to Neogene in the paleo-Indus repository upstream of the confluence, the proportion of Indian plate material increases in the downstream repositories, at the Eocene–Oligocene boundary in the paleodelta, and in the mid-Eocene in the Indus Fan. More research is required to understand the reasons for this discrepancy in timing of the shift in the downstream repositories, but nevertheless we can conclude that the Punjabi tributary system joined the paleo-Indus trunk river at or before the start of the Oligocene.

REFERENCES CITED

Abbasi, I.A., and Friend, P.F., 1989, Uplift and evolution of the Himalayan orogenic belts, as recorded in the foredeep molasse sediments: Zeitschrift für Geomorphologie, NF Supplementband 76, p. 75–88.

Ahmad, T., Harris, N., Bickle, M., Chapman, H., Bunbury, J., and Prince, C., 2000, Isotopic constraints on the structural relationships between the lesser Himalayan series and the high Himalayan crystalline series, Garhwal Himalaya: Geological Society of America Bulletin, v. 112, p. 467–477, https://doi.org/10.1130/0016-7606(2000)112<467:ICOTSR>2.0.CO;2.

Aitchison, J.C., Ali, J.R., and Davis, A.M., 2007, When and where did India and Asia collide?: Journal of Geophysical Research: Solid Earth, v. 112, p. 1–19.

Alizai, A., Carter, A., Clift, P.D., VanLaningham, S., Williams, J.C., and Kumar, R., 2011, Sediment provenance, reworking and transport processes in the Indus River by U–Pb dating of detrital zircon grains: Global and Planetary Change, v. 76, p. 33–55, https://doi.org/10.1016/j.gloplacha.2010.11.008.

Andò, S., Aharonovich, S., Hahn, A., George, S., Clift, P., and Garzanti, E., 2020, Integrating heavy-mineral, geochemical and biomarker analyses of Plio-Pleistocene sandy and silty turbidites: A novel approach for provenance studies (Indus Fan, IODP Expedition 355): Geological Magazine, v. 157, p. 929–938, https://doi.org/10.1017/S0016756819000773.

Argles, T., Foster, G., Whittington, A., Harris, N., and George, M., 2003, Isotope studies reveal a complete Himalayan section in the Nanga Parbat syntaxis: Geology, v. 31, p. 1109–1112, https://doi.org/10.1130/G19937.1.

Awais, M., Qasim, M., Tanoli, J.I., Ding, L., Sattar, M., Baig, M.S., and Pervaiz, S., 2021, Detrital zircon provenance of the Cenozoic sequence, Kotli, Northwestern Himalaya, Pakistan; Implications for India–Asia Collision: Minerals, v. 11, https://doi.org/10.3390/min11121399.

Baig, M.S., and Munir, M.-u.-H., 2007, Foraminiferal biostratigraphy of Yadgar area, Muzaffarabad Azad Kashmir, Pakistan: Journal of Himalayan Earth Sciences, v. 40.

Bernet, M., van der Beek, P., Pik, R., Huyghe, P., Mugnier, J.L., Labrin, E., and Szulc, A., 2006, Miocene to Re-

cent exhumation of the central Himalaya determined from combined detrital zircon fission-track and U/Pb analysis of Siwalik sediments, western Nepal: Basin Research, v. 18, p. 393–412, https://doi.org/10.1111/j .1365-2117.2006.00303.x.

Bhattacharya, G., Robinson, D.M., and Wielicki, M.M., 2021, Detrital zircon provenance of the Indus Group, Ladakh, NW India: Implications for the timing of the India-Asia collision and other syn-orogenic processes: Geological Society of America Bulletin, v. 133, p. 1007–1020, https://doi.org/10.1130/B35624.1.

Bignold, S., and Treloar, P., 2003, Northward subduction of the Indian Plate beneath the Kohistan island arc, Pakistan Himalaya: New evidence from isotopic data: Journal of the Geological Society, v. 160, p. 377–384, https://doi.org/10.1144/0016-764902-068.

Bossart, P., and Ottiger, R., 1989, Rocks of the Murree Formation in northern Pakistan: Indicators of a descending foreland basin of late Paleocene to middle Eocene age: Eclogae Geologicae Helvetiae, v. 82, p. 133–165.

Bouilhol, P., Jagoutz, O., Hanchar, J.M., and Dudas, F.O., 2013, Dating the India–Eurasia collision through arc magmatic records: Earth and Planetary Science Letters, v. 366, p. 163–175, https://doi.org/10.1016/j.epsl.2013 .01.023.

Burbank, D.W., and Tahirkheli, R.K., 1985, The magnetostratigraphy, fission-track dating, and stratigraphic evolution of the Peshawar intermontane basin, northern Pakistan: Geological Society of America Bulletin, v. 96, p. 539–552, https://doi.org/10.1130 /0016-7606(1985)96<539:TMFDAS>2.0.CO;2.

Burbank, D.W., Beck, R.A., and Mulder, T., 1996, The Himalayan foreland basin, *in* Yin, A., and Harrison, M., eds., The Tectonic Evolution of Asia: Cambridge, UK, Cambridge University Press, p. 149–190.

Carter, A., Najman, Y., Bahroudi, A., Bown, P., Garzanti, E., and Lawrence, R.D., 2010, Locating earliest records of orogenesis in western Himalaya: Evidence from Paleogene sediments in the Iranian Makran region and Pakistan Katawaz basin: Geology, v. 38, p. 807–810, https://doi.org/10.1130/G31087.1.

Cerveny, P., Johnson, N., Tahirkheli, R., and Bonis, N., 1989, Tectonic and geomorphic implications of Siwalik Group heavy minerals, *in* Malinconico, L.L., Jr., and Lillie, R.J., eds., Tectonics of Western Himalayas: Geological Society of America Special Paper 232, p. 129–136, https://doi.org/10.1130/SPE232-p129.

Chirouze, F., Huyghe, P., Chauvel, C., van der Beek, P., Bernet, M., and Mugnier, J.-L., 2015, Stable drainage pattern and variable exhumation in the Western Himalaya since the middle Miocene: The Journal of Geology, v. 123, p. 1–20, https://doi.org/10.1086/679305.

Clift, P.D., and Blusztajn, J., 2005, Reorganization of the western Himalayan river system after five million years ago: Nature, v. 438, p. 1001–1003, https://doi.org/10 .1038/nature04379.

Clift, P.D., Shimizu, N., Layne, G.D., Blusztajn, J.S., Gaedicke, C., Schlüter, H.-U., Clark, M.K., and Amjad, S., 2001a, Development of the Indus Fan and its significance for the erosional history of the Western Himalaya and Karakoram: Geological Society of America Bulletin, v. 113, p. 1039–1051, https://doi.org/10.1130 /0016-7606(2001)113<1039:DOTIFA>2.0.CO;2.

Clift, P.D., Shimizu, N., Layne, G., and Blusztajn, J., 2001b, Tracing patterns of unroofing in the Early Himalaya through microprobe Pb isotope analysis of detrital K-feldspars in the Indus Molasse, India: Earth and Planetary Science Letters, v. 188, p. 475–491, https://doi.org /10.1016/S0012-821X(01)00346-6.

Clift, P.D., Carter, A., Krol, M., and Kirby, E., 2002a, Constraints on India-Eurasia collision in the Arabian Sea region taken from the Indus Group, Ladakh Himalaya, India, *in* Clift, P.D., Kroon, D., Gaedicke, C., and Craig, J., eds., The Tectonic and Climatic Evolution of the Arabian Sea Region: Geological Society, London, Special Publication 195, p. 97–116, https://doi.org/10 .1144/GSL.SP.2002.195.01.01.

Clift, P.D., Lee, J.I., Hildebrand, P., Shimizu, N., Layne, G.D., Blusztajn, J., Blum, J.D., Garzanti, E., and Khan, A.A., 2002b, Nd and Pb isotope variability in the Indus River System: Implications for sediment provenance and crustal heterogeneity in the Western Himalaya:

Earth and Planetary Science Letters, v. 200, p. 91–106, https://doi.org/10.1016/S0012-821X(02)00620-9.

Clift, P.D., Campbell, I.H., Pringle, M.S., Carter, A., Zhang, X., Hodges, K.V., Khan, A.A., and Allen, C.M., 2004, Thermochronology of the modern Indus River bedload: New insight into the controls on the marine stratigraphic record: Tectonics, v. 23, https://doi.org/10.1029 /2003TC001559.

Clift, P.D., Carter, A., and Jonell, T.N., 2014, U–Pb dating of detrital zircon grains in the Paleocene Stumpata Formation, Tethyan Himalaya, Zanskar, India: Journal of Asian Earth Sciences, v. 82, p. 80–89, https://doi.org/10 .1016/j.jseaes.2013.12.014.

Clift, P.D., Zhou, P., Stockli, D.F., and Blusztajn, J., 2019, Regional Pliocene exhumation of the Lesser Himalaya in the Indus drainage: Solid Earth, v. 10, p. 647–661, https://doi.org/10.5194/se-10-647-2019.

Clift, P.D., Mark, C., Alizai, A., Khan, H., and Jan, M.Q., 2022, Detrital U–Pb rutile and zircon data show Indus River sediment dominantly eroded from East Karakoram, not Nanga Parbat: Earth and Planetary Science Letters, v. 600, https://doi.org/10.1016/j.epsl.2022.117873.

Coward, M., Jan, Q., Rex, D., Tarney, J., and Thirwall, M., 1984, Geology of the south central Karakoram and Kohistan, *in* Miller, K.J., ed., The International Karakoram Project, Volume 2: Cambridge, UK, Cambridge University Press, p. 71–85.

DeCelles, P.G., Gehrels, G.E., Quade, J., and Ojha, T., 1998, Eocene–early Miocene foreland basin development and the history of Himalayan thrusting, western and central Nepal: Tectonics, v. 17, p. 741–765, https://doi.org/10 .1029/98TC02598.

DeCelles, P.G., Gehrels, G.E., Najman, Y., Martin, A.J., Carter, A., and Garzanti, E., 2004, Detrital geochronology and geochemistry of Cretaceous–early Miocene strata of Nepal: Implications for timing and diachroneity of initial Himalayan orogenesis: Earth and Planetary Science Letters, v. 227, p. 313–330, https://doi.org/10 .1016/j.epsl.2004.08.019.

DeCelles, P.G., Carrapa, B., Gehrels, G.E., Chakraborty, T., and Ghosh, P., 2016, Along-strike continuity of structure, stratigraphy, and kinematic history in the Himalayan thrust belt: The view from Northeastern India: Tectonics, v. 35, p. 2995–3027, https://doi.org/10.1002 /2016TC004298.

DeCelles, P.G., Castañeda, I.S., Carrapa, B., Liu, J., Quade, J., Leary, R., and Zhang, L., 2018, Oligocene–Miocene Great Lakes in the India-Asia Collision Zone: Basin Research, v. 30, p. 228–247, https://doi.org/10.1111 /bre.12217.

Deniel, C., Vidal, P., Fernandez, A., Le Fort, P., and Peucat, J.-J., 1987, Isotopic study of the Manaslu granite (Himalaya, Nepal): Inferences on the age and source of Himalayan leucogranites: Contributions to Mineralogy and Petrology, v. 96, p. 78–92, https://doi.org/10.1007 /BF00375529.

Ding, H., Zhang, Z., Dong, X., Tian, Z., Xiang, H., Mu, H., Gou, Z., Shui, X., Li, W., and Mao, L., 2016a, Early Eocene (c. 50 Ma) collision of the Indian and Asian continents: Constraints from the North Himalaya metamorphic rocks, southeastern Tibet: Earth and Planetary Science Letters, v. 435, p. 64–73, https://doi.org /10.1016/j.epsl.2015.12.006.

Ding, L., Qasim, M., Jadoon, I.A., Khan, M.A., Xu, Q., Cai, F., Wang, H., Baral, U., and Yue, Y., 2016b, The India–Asia collision in north Pakistan: Insight from the U–Pb detrital zircon provenance of Cenozoic foreland basin: Earth and Planetary Science Letters, v. 455, p. 49–61, https://doi.org/10.1016/j.epsl.2016.09.003.

DiPietro, J.A., Hussain, A., Ahmad, I., and Khan, M.A., 2000, The main mantle thrust in Pakistan: Its character and extent, *in* Khan, M.A., Treloar, P.J., Searle, M.P., and Qasim Jan, M., eds., Tectonics of the Nanga Parbat Syntaxis and the Western Himalaya: Geological Society, London, Special Publication 170, p. 375–393, https://doi.org/10.1144/GSL.SP.2000.170.01.20.

DiPietro, J.A., and Pogue, K.R., 2004, Tectonostratigraphic subdivisions of the Himalaya: A view from the west: Tectonics, v. 23, https://doi.org/10.1029 /2003TC001554.

DiPietro, J.A., Ahmad, I., and Hussain, A., 2008, Cenozoic kinematic history of the Kohistan fault in the Paki-

stan Himalaya: Geological Society of America Bulletin, v. 120, p. 1428–1440, https://doi.org/10.1130 /B26204.1.

DiPietro, J.A., Pullen, A., and Krol, M.A., 2021, Geologic history and thermal evolution in the hinterland region, western Himalaya, Pakistan: Earth-Science Reviews, v. 223, https://doi.org/10.1016/j.earscirev.2021.103817.

Dunlap, W.J., Weinberg, R.F., and Searle, M.P., 1998, Karakoram fault zone rocks cool in two phases: Journal of the Geological Society, v. 155, p. 903–912, https://doi .org/10.1144/gsjgs.155.6.0903.

Exnicios, E.M., Carter, A., Najman, Y., and Clift, P.D., 2022, Late Miocene unroofing of the Inner Lesser Himalaya recorded in the NW Himalaya foreland basin: Basin Research, v. 34, p. 1894–1916, https://doi.org/10.1111 /bre.12689.

Feng, H., Lu, H., Carrapa, B., Zhang, H., Chen, J., Wang, Y., and Clift, P.D., 2021, Erosion of the Himalaya-Karakoram recorded by Indus Fan deposits since the Oligocene: Geology, v. 49, p. 1126–1131, https://doi .org/10.1130/G48445.1.

Fraser, J.E., Searle, M.P., Parrish, R.R., and Noble, S.R., 2001, Chronology of deformation, metamorphism, and magmatism in the southern Karakoram Mountains: Geological Society of America Bulletin, v. 113, p. 1443–1455, https://doi.org/10.1130 /0016-7606(2001)113<1443:CODMAM>2.0;2.

Gaetani, M., and Garzanti, E., 1991, Multicyclic history of the Northern India continental margin (Northwestern Himalaya)(1): AAPG Bulletin, v. 75, p. 1427–1446.

Gaetani, M., Jadoul, F., Erba, E., and Garzanti, E., 1993, Jurassic and Cretaceous orogenic events in the North Karakoram: Age constraints from sedimentary rocks, *in* Treolar, P.J., and Searles, M.P., eds., Himalayan Tectonics: Geological Society, London, Special Publication 74, p. 39–52, https://doi.org/10.1144/GSL.SP.1993.074 .01.04.

Garzanti, E., and Andò, S., 2019, Heavy minerals for junior woodchucks: Minerals, v. 9, no. 3, p. 148, https://doi .org/10.3390/min9030148.

Garzanti, E., Andò, S., and Vezzoli, G., 2009, Grain-size dependence of sediment composition and environmental bias in provenance studies: Earth and Planetary Science Letters, v. 277, p. 422–432, https://doi.org/10.1016/j .epsl.2008.11.007.

Garzanti, E., Andò, S., and Vezzoli, G., 2020, Provenance of Cenozoic Indus Fan sediments (IODP Sites U1456 and U1457): Journal of Sedimentary Research, v. 90, p. 1114–1127, https://doi.org/10.2110/jsr.2019-195.

Gehrels, G., Kapp, P., DeCelles, P., Pullen, A., Blakey, R., Weislogel, A., Ding, L., Guynn, J., Martin, A., and McQuarrie, N., 2011, Detrital zircon geochronology of pre-Tertiary strata in the Tibetan-Himalayan orogen: Tectonics, v. 30, https://doi.org/10.1029 /2011TC002868.

Henderson, A.L., Najman, Y., Parrish, R., BouDagher-Fadel, M., Barford, D., Garzanti, E., and Andò, S., 2010, Geology of the Cenozoic Indus Basin sedimentary rocks: Paleoenvironmental interpretation of sedimentation from the western Himalaya during the early phases of India-Eurasia collision: Tectonics, v. 29, https://doi.org /10.1029/2009TC002651.

Henderson, A.L., Najman, Y., Parrish, R., Mark, D.F., and Foster, G.L., 2011, Constraints to the timing of India–Eurasia collision; a re-evaluation of evidence from the Indus Basin sedimentary rocks of the Indus–Tsangpo Suture Zone, Ladakh, India: Earth-Science Reviews, v. 106, p. 265–292, https://doi.org/10.1016/j.earscirev .2011.02.006.

Hildebrand, P., Noble, S., Searle, M., and Parrish, R., 1998, Tectonic significance of 24 Ma crustal melting in the eastern Hindu Kush, Pakistan: Geology, v. 26, p. 871–874, https://doi.org/10.1130 /0091-7613(1998)026<0871:TSOMCM>2.3.CO;2.

Hildebrand, P., Noble, S., Searle, M., Waters, D., and Parrish, R., 2001, Old origin for an active mountain range: Geology and geochronology of the eastern Hindu Kush, Pakistan: Geological Society of America Bulletin, v. 113, p. 625–639, https://doi.org/10.1130 /0016-7606(2001)113<0625:OOFAAM>2.0.CO;2.

Hodges, K.V., 2000, Tectonics of the Himalaya and southern Tibet from two perspectives: Geological Society

of America Bulletin, v. 112, p. 324–350, https://doi .org/10.1130/0016-7606(2000)112<324:TOTHAS>2 .0.CO;2.

Hu, X., Garzanti, E., Wang, J., Huang, W., An, W., and Webb, A., 2016, The timing of India-Asia collision onset— Facts, theories, controversies: Earth-Science Reviews, v. 160, p. 264–299, https://doi.org/10.1016/j.earscirev .2016.07.014.

Ji, W., Wu, F., Liu, C., and Chung, S., 2009, Geochronology and petrogenesis of granitic rocks in Gangdese Batholith, southern Tibet: Science in China Series D: Earth Sciences, v. 52, p. 1240–1261, https://doi.org/10.1007 /s11430-009-0131-y.

Johnson, N.M., Stix, J., Tauxe, L., Cerveny, P.F., and Tahirkheli, R.A., 1985, Paleomagnetic chronology, fluvial processes, and tectonic implications of the Siwalik deposits near Chinji Village, Pakistan: The Journal of Geology, v. 93, p. 27–40, https://doi.org/10 .1086/628917.

Jonell, T.N., Li, Y., Blusztajn, J., Giosan, L., and Clift, P.D., 2018, Signal or noise?: Isolating grain size effects on Nd and Sr isotope variability in Indus delta sediment provenance: Chemical Geology, v. 485, p. 56–73, https://doi.org/10.1016/j.chemgeo.2018.03.036.

Khan, M.A., Stern, R.J., Gribble, R.F., and Windley, B.F., 1997, Geochemical and isotopic constraints on subduction polarity, magma sources, and palaeogeography of the Kohistan intra-oceanic arc, northern Pakistan Himalaya: Journal of the Geological Society, v. 154, p. 935–946, https://doi.org/10.1144/gsjgs.154.6.0935.

Khan, S.D., Stern, R.J., Manton, M.I., Copeland, P., Kinnana, J.I., and Khan, M.A., 2004, Age, geochemical and Sr– Nd–Pb isotopic constraints for mantle source characteristics and petrogenesis of Teru Volcanics, Northern Kohistan Terrane, Pakistan: Tectonophysics, v. 393, p. 263–280, https://doi.org/10.1016/j.tecto.2004.07 .038.

Khan, S.D., Walker, D.J., Hall, S.A., Burke, K.C., Shah, M.T., and Stockli, L., 2009, Did the Kohistan-Ladakh island arc collide first with India?: Geological Society of America Bulletin, v. 121, p. 366–384, https://doi.org /10.1130/B26348.1.

Koppers, A.A., 2002, ArArCALC—Software for $^{40}Ar/^{39}Ar$ age calculations: Computers & Geosciences, v. 28, p. 605–619, https://doi.org/10.1016/S0098 -3004(01)00095-4.

Leier, A.L., Kapp, P., Gehrels, G.E., and DeCelles, P.G., 2007, Detrital zircon geochronology of Carboniferous–Cretaceous strata in the Lhasa terrane, Southern Tibet: Basin Research, v. 19, p. 361–378, https://doi.org /10.1111/j.1365-2117.2007.00330.x.

Mahéo, G., Blichert-Toft, J., Pin, C., Guillot, S., and Pêcher, A., 2009, Partial melting of mantle and crustal sources beneath South Karakorum, Pakistan: Implications for the Miocene geodynamic evolution of the India–Asia convergence zone: Journal of Petrology, v. 50, p. 427– 449, https://doi.org/10.1093/petrology/egp006.

Malusà, M.G., Resentini, A., and Garzanti, E., 2016, Hydraulic sorting and mineral fertility bias in detrital geochronology: Gondwana Research, v. 31, p. 1–19, https://doi .org/10.1016/j.gr.2015.09.002.

Miller, C., Schuster, R., Klötzli, U., Frank, W., and Purtscheller, F., 1999, Post-collisional potassic and ultrapotassic magmatism in SW Tibet: Geochemical and Sr–Nd–Pb–O isotopic constraints for mantle source characteristics and petrogenesis: Journal of Petrology, v. 40, p. 1399–1424, https://doi.org/10.1093/petroj/40 .9.1399.

Najman, Y., 2006, The detrital record of orogenesis: A review of approaches and techniques used in the Himalayan sedimentary basins: Earth-Science Reviews, v. 74, p. 1–72.

Najman, Y., Pringle, M., Godin, L., and Oliver, G., 2001, Dating of the oldest continental sediments from the Himalayan foreland basin: Nature, v. 410, p. 194–197, https://doi.org/10.1038/35065577.

Najman, Y., Pringle, M., Godin, L., and Oliver, G., 2002, A reinterpretation of the Balakot Formation: Implications for the tectonics of the NW Himalaya, Pakistan: Tectonics, v. 21, p. 9-1–9-18.

Najman, Y., Garzanti, E., Pringle, M., Bickle, M., Stix, J., and Khan, I., 2003, Early–middle Miocene paleodrainage

and tectonics in the Pakistan Himalaya: Geological Society of America Bulletin, v. 115, p. 1265–1277, https:// doi.org/10.1130/B25165.1.

Najman, Y., Bickle, M., Garzanti, E., Pringle, M., Barfod, D., Brozovic, N., Burbank, D., and Ando, S., 2009, Reconstructing the exhumation history of the Lesser Himalaya, NW India, from a multitechnique provenance study of the foreland basin Siwalik Group: Tectonics, v. 28, https://doi.org/10.1029/2009TC002506.

Nyberg, B., Helland-Hansen, W., Gawthorpe, R.L., Sandbakken, P., Eide, C.H., Sømme, T., Hadler-Jacobsen, F., and Leiknes, S., 2018, Revisiting morphological relationships of modern source-to-sink segments as a first-order approach to scale ancient sedimentary systems: Sedimentary Geology, v. 373, p. 111–133, https://doi.org /10.1016/j.sedgeo.2018.06.007.

Palin, R., Searle, M., Waters, D., Horstwood, M., and Parrish, R., 2012, Combined thermobarometry and geochronology of peraluminous metapelites from the Karakoram metamorphic complex, North Pakistan; New insight into the tectonothermal evolution of the Baltoro and Hunza Valley regions: Journal of Metamorphic Geology, v. 30, p. 793–820, https://doi.org /10.1111/j.1525-1314.2012.00999.x.

Pan, F.-B., Zhang, H.-F., Xu, W.-C., Guo, L., Wang, S., and Luo, B.-j., 2014, U–Pb zircon chronology, geochemical and Sr–Nd isotopic composition of Mesozoic–Cenozoic granitoids in the SE Lhasa terrane: Petrogenesis and tectonic implications: Lithos, v. 192–195, p. 142–157, https://doi.org/10.1016/j.lithos.2014.02.005.

Pivnik, D.A., and Wells, N.A., 1996, The transition from Tethys to the Himalaya as recorded in northwest Pakistan: Geological Society of America Bulletin, v. 108, p. 1295–1313, https://doi.org/10.1130 /0016-7606(1996)108<1295:TTFTTT>2.3.CO;2.

Qasim, M., Ding, L., Khan, M.A., Jadoon, I.A., Haneef, M., Baral, U., Cai, F., Wang, H., and Yue, Y., 2018, Tectonic implications of detrital zircon ages from lesser Himalayan Mesozoic–Cenozoic strata, Pakistan: Geochemistry, Geophysics, Geosystems, v. 19, p. 1636–1659, https://doi.org/10.1002/2017GC006895.

Qayyum, M., Niem, A.R., and Lawrence, R.D., 2001, Detrital modes and provenance of the Paleogene Khojak Formation in Pakistan: Implications for early Himalayan orogeny and unroofing: Geological Society of America Bulletin, v. 113, p. 320–332, https://doi.org/10.1130 /0016-7606(2001)113<0320:DMAPOT>2.0.CO;2.

Richards, A., Argles, T., Harris, N., Parrish, R., Ahmad, T., Darbyshire, F., and Draganits, E., 2005, Himalayan architecture constrained by isotopic tracers from clastic sediments: Earth and Planetary Science Letters, v. 236, p. 773–796, https://doi.org/10.1016/j .epsl.2005.05.034.

Robinson, D.M., DeCelles, P.G., Patchett, P.J., and Garzione, C.N., 2001, The kinematic evolution of the Nepalese Himalaya interpreted from Nd isotopes: Earth and Planetary Science Letters, v. 192, p. 507–521, https://doi.org /10.1016/S0012-821X(01)00451-4.

Roddaz, M., Said, A., Guillot, S., Antoine, P.-O., Montel, J.-M., Martin, F., and Darrozes, J., 2011, Provenance of Cenozoic sedimentary rocks from the Sulaiman fold and thrust belt, Pakistan: Implications for the palaeogeography of the Indus drainage system: Journal of the Geological Society, v. 168, p. 499–516, https://doi.org /10.1144/0016-76492010-100.

Schaltegger, U., Zeilinger, G., Frank, M., and Burg, J.P., 2002, Multiple mantle sources during island arc magmatism: U–Pb and Hf isotopic evidence from the Kohistan arc complex, Pakistan: Terra Nova, v. 14, p. 461–468, https://doi.org/10.1046/j.1365-3121.2002 .00432.x.

Schärer, U., Hamet, J., and Allègre, C.J., 1984, The Transhimalaya (Gangdese) plutonism in the Ladakh region: A U-Pb and Rb-Sr study: Earth and Planetary Science Letters, v. 67, p. 327–339, https://doi.org/10.1016 /0012-821X(84)90172-9.

Schneider, D., Zeitler, P., Kidd, W., and Edwards, M., 2001, Geochronologic constraints on the tectonic evolution and exhumation of Nanga Parbat, western Himalaya syntaxis, revisited: The Journal of Geology, v. 109, p. 563–583, https://doi.org/10.1086 /322764.

Searle, M., Khan, M.A., Fraser, J., Gough, S., and Jan, M.Q., 1999, The tectonic evolution of the Kohistan-Karakoram collision belt along the Karakoram Highway transect, north Pakistan: Tectonics, v. 18, p. 929–949, https://doi.org/10.1029/1999TC900042.

Searle, M., Parrish, R.R., Thow, A., Noble, S., Phillips, R., and Waters, D., 2010, Anatomy, age and evolution of a collisional mountain belt: The Baltoro granite batholith and Karakoram Metamorphic Complex, Pakistani Karakoram: Journal of the Geological Society, v. 167, p. 183–202, https://doi.org/10.1144 /0016-76492009-043.

Shah, S.I., 2009, Stratigraphy of Pakistan: Geological Survey of Pakistan Memoir 22.

Sinclair, H., and Jaffey, N., 2001, Sedimentology of the Indus Group, Ladakh, northern India: Implications for the timing of initiation of the palaeo-Indus River: Journal of the Geological Society, v. 158, p. 151–162, https:// doi.org/10.1144/jgs.158.1.151.

Treloar, P., Rex, D., Guise, P., Wheeler, J., Hurford, A., and Carter, A., 2000, Geochronological constraints on the evolution of the Nanga Parbat syntaxis, Pakistan Himalaya, *in* Khan, M.A., Treloar, P.J., Searle, M.P., and Qasim Jan, M., eds., Tectonics of the Nanga Parbat Syntaxis and the Western Himalaya: Geological Society, London, Special Publication 170, p. 137–162, https:// doi.org/10.1144/GSL.SP.2000.170.01.08.

Treloar, P.J., Palin, R.M., and Searle, M.P., 2019, Towards resolving the metamorphic enigma of the Indian Plate in the NW Himalaya of Pakistan, *in* Treloar, P.J., and Searle, M.P., eds., Himalayan Tectonics: A Modern Synthesis: Geological Society, London, Special Publication 483, p. 255–279, https://doi.org/10.1144 /SP483-2019-22.

Ullah, K., Arif, M., and Shah, M.T., 2015, Geochemistry and provenance of the Lower Siwaliks from southwestern Kohat, western Himalayan Foreland Basin, NW Pakistan: Geologica Acta: An International Earth Science Journal, v. 13, p. 45–61.

van der Beek, P., Van Melle, J., Guillot, S., Pêcher, A., Reiners, P.W., Nicolescu, S., and Latif, M., 2009, Eocene Tibetan plateau remnants preserved in the northwest Himalaya: Nature Geoscience, v. 2, p. 364–368, https:// doi.org/10.1038/ngeo503.

van Hinsbergen, D.J., Lippert, P.C., Dupont-Nivet, G., McQuarrie, N., Doubrovine, P.V., Spakman, W., and Torsvik, T.H., 2012, Greater India Basin hypothesis and a two-stage Cenozoic collision between India and Asia: Proceedings of the National Academy of Sciences of the United States of America, v. 109, p. 7659–7664, https://doi.org/10.1073/pnas.1117262109.

Wallis, D., Carter, A., Phillips, R.J., Parsons, A.J., and Searle, M.P., 2016, Spatial variation in exhumation rates across Ladakh and the Karakoram: New apatite fission track data from the Eastern Karakoram, NW India: Tectonics, v. 35, p. 704–721, https://doi.org/10.1002 /2015TC003943.

Welcomme, J.-L., Benammi, M., Crochet, J.-Y., Marivaux, L., Métais, G., Antoine, P.-O., and Baloch, I., 2001, Himalayan Forelands: Palaeontological evidence for Oligocene detrital deposits in the Bugti Hills (Balochistan, Pakistan): Geological Magazine, v. 138, p. 397–405, https://doi.org/10.1017/S0016756801005428.

Whittington, A., Foster, G., Harris, N., Vance, D., and Ayres, M., 1999, Lithostratigraphic correlations in the western Himalaya—An isotopic approach: Geology, v. 27, p. 585–588, https://doi.org/10.1130 /0091-7613(1999)027<0585:LCITWH>2.3.CO;2.

Willis, B., 1993, Evolution of Miocene fluvial systems in the Himalayan foredeep through a two kilometerthick succession in northern Pakistan: Sedimentary Geology, v. 88, p. 77–121, https://doi.org/10.1016 /0037-0738(93)90152-U.

Yeats, R.S., and Hussain, A., 1987, Timing of structural events in the Himalayan foothills of northwestern Pakistan: Geological Society of America Bulletin, v. 99, p. 161–176, https://doi.org/10.1130 /0016-7606(1987)99<161:TOSEIT>2.0.CO;2.

Yu, Z., Colin, C., Wan, S., Saraswat, R., Song, L., Xu, Z., Clift, P., Lu, H., Lyle, M., and Kulhanek, D., 2019, Sea level-controlled sediment transport to the eastern Arabian Sea over the past 600 kyr: Clay minerals and Sr-Nd

isotopic evidence from IODP site U1457: Quaternary Science Reviews, v. 205, p. 22–34, https://doi.org/10.1016/j.quascirev.2018.12.006.

Zaleha, M.J., 1997, Intra- and extrabasinal controls on fluvial deposition in the Miocene Indo-Gangetic foreland basin, northern Pakistan: Sedimentology, v. 44, p. 369–390, https://doi.org/10.1111/j.1365-3091.1997.tb01530.x.

Zanchi, A., and Gaetani, M., 2011, The geology of the Karakoram range, Pakistan: The new 1:100,000 geological map of Central-Western Karakoram: Italian Journal of Geosciences, v. 130, p. 161–262.

Zhang, H., Harris, N., Parrish, R., Kelley, S., Zhang, L., Rogers, N., Argles, T., and King, J., 2004, Causes and consequences of protracted melting of the mid-crust exposed in the North Himalayan antiform: Earth and Planetary Science Letters, v. 228, p. 195–212, https://doi.org/10.1016/j.epsl.2004.09.031.

Zhou, P., Stockli, D.F., Ireland, T., Murray, R.W., and Clift, P.D., 2021, Zircon U-Pb age constraints on NW Hima-layan exhumation from the Laxmi Basin, Arabian Sea: Geochemistry, Geophysics, Geosystems, v. 23, https://doi.org/10.1029/2021GC010158.

Zhu, D.-C., Mo, X.-X., Niu, Y., Zhao, Z.-D., Wang, L.-Q., Liu, Y.-S., and Wu, F.-Y., 2009, Geochemical investigation of Early Cretaceous igneous rocks along an east–west traverse throughout the central Lhasa Terrane, Tibet: Chemical Geology, v. 268, p. 298–312, https://doi.org/10.1016/j.chemgeo.2009.09.008.

Zhu, D.-C., Zhao, Z.-D., Niu, Y., Dilek, Y., Wang, Q., Ji, W.-H., Dong, G.-C., Sui, Q.-L., Liu, Y.-S., and Yuan, H.-L., 2012, Cambrian bimodal volcanism in the Lhasa Terrane, southern Tibet: Record of an early Paleozoic Andean-type magmatic arc in the Australian proto-Tethyan margin: Chemical Geology, v. 328, p. 290–308, https://doi.org/10.1016/j.chemgeo.2011.12.024.

Zhuang, G., Najman, Y., Guillot, S., Roddaz, M., Antoine, P.-O., Métais, G., Carter, A., Marivaux, L., and So-langi, S.H., 2015, Constraints on the collision and the pre-collision tectonic configuration between India and Asia from detrital geochronology, thermo-chronology, and geochemistry studies in the Lower Indus Basin, Pakistan: Earth and Planetary Science Letters, v. 432, p. 363–373, https://doi.org/10.1016/j.epsl.2015.10.026.

Zhuang, G., Najman, Y., Tian, Y., Carter, A., Gemignani, L., Wijbrans, J., Jan, M.Q., and Khan, M.A., 2018, Insights into the evolution of The Hindu Kush-Kohistan-Karakoram from modern river sand detrital geo- and thermochronological studies: Journal of the Geological Society, v. 175, p. 934–948.